Contemporary Atmospheric Escape at Mars: Implications for Astrobiology

D.A. Brain[1], J.G. Luhmann[2], C.T. Russell[3]

Corresponding Author: D.A. Brain

Address: UCB 392 / Boulder, CO 80309-0392

Phone: 303 492-3395

Fax: 303 492-6946

e-mail: david.brain@colorado.edu

Running Title: BRAIN ET AL.: MARTIAN ATMOSPHERIC ESCAPE

Keywords:

DRAFT FOR SUBMISSION TO ASTROBIOLOGY

[1]Laboratory for Atmospheric and Space Physics, University of Colorado at Boulder, Boulder, CO 80309-0392

[2]Space Science Lab, University of California at Berkeley

[3]Institute of Geophysics and Planetary Physics, University of California Los Angeles

Abstract

The development of life on Earth is believed to have resulted in permanent changes in the composition of the atmosphere. A search for atmospheric biosignatures is one of the major objectives of the powerful telescopes currently being designed to search for terrestrial extrasolar planets. In our own solar system, Mars is considered one of the best candidates for the development of life. However, identification of an atmospheric biosignature on Mars is not possible until all potential abiotic processes have been accounted for. At present we are particularly limited by our understanding of the role of atmospheric escape at Mars through its history. This paper summarizes the present understanding of the physics of atmospheric escape to space at Mars, discusses the constraints on the estimates of loss (both at present and over Martian history), suggests important measurements and model improvements that would significantly improve our understanding of this important process, and relates the current understanding to the possibility of detection of an atmospheric biosignature.

Introduction

With the discovery of more than 100 extra-solar planets in the past decade, increased attention has been given to possible methods of remote detection of biological activity on planetary bodies [*Des Marais et al.*, 2002]. It is well-accepted that the presence of life has affected Earth's atmosphere [e.g. *Wayne*, 1992]. Therefore, one promising type of observation is of disequilibria in atmospheric composition, chemistry or temperature [*Lederberg*, 1965; *Lovelock*, 1965]. Such methods have not yet been exploited in attempts to detect life on other planets in our solar system [*Sagan et al.*, 1993]. The Martian atmosphere in particular could be studied for global or local biosignatures of subsurface life [*Summers et al.*, 2002]. However, unambiguous detection of extant (or extinct) life is only possible after the contributions of the many abiotic processes at work on Mars have been understood, quantified, and eliminated. Part of the procedure for determining disequilibrium conditions is understanding the abiotic interaction of the atmosphere with its boundaries. For example, surface liquid water can remove substantial amounts of CO_2, as in the case of Earth [*Pollack*, 1979], while loss or accretion from the upper boundary can measurably alter composition and isotope ratios, as in the case of the D/H ratio at Venus [*Donahue et al.*, 1982]. The effects of these processes are of course accumulated over time.

The Martian atmosphere is thin and cold today, relative to the atmospheres of Earth and Venus, but this has probably not always been the case. Geologic features (dendritic valley networks, lack of small craters) indicate that the Martian atmosphere was at one time capable of supporting liquid water at the surface for substantial periods of time [*Jakosky and Phillips*, 2001, and refs. therein]. Since the Martian atmosphere is currently incapable of supporting liquid water [*Jakosky and Haberle*, 1992], we know that atmospheric sinks have played an important role in the evolution of the Martian climate. Several of the many atmospheric sources and sinks are shown in Figure 1. Of the possible loss processes that acted and/or are acting at Mars, escape to space is the one process by which atmospheric particles are permanently removed from the planet. Escape to space is likely the major loss process acting today, and has played a significant role in atmospheric evolution over Martian history.

Here we review current understanding of atmospheric escape at Mars, including the processes that are acting today, our knowledge of the current escape rates, and atmospheric escape over Martian history. We discuss the major questions that remain to be addressed, and suggest measurements and modeling efforts for an improved understanding of escape. We also relate the current understanding to the goal of detection of an atmospheric biosignature.

Current Understanding

Solar Wind Interaction

The solar wind interaction at Mars is particularly relevant to the study of atmospheric escape. Mars' small size (and mass) mean that the atmosphere is more extended (relative to planetary radius) than planets like Venus or Earth. Moreover, because Mars lacks a protective global magnetic field, this extended atmosphere interacts directly with the solar wind, with the result that upper atmospheric particles are continuously removed [*Michel*, 1971]. The Martian exobase is typically observed around 190 km, and plasma dominated by shocked solar wind electrons has been observed at altitudes as low as 170 km [*Mitchell et al.*, 2001]). Above the exobase collisions are unimportant. Any neutral atom or molecule that is moving with a velocity greater than the escape velocity of ~ 5 km/s and is on an escape trajectory can leave the planet. Similarly, as will be discussed below, any ion produced in the atmosphere above the ionopause can be removed by the solar wind regardless of its initial velocity or direction, provided that it is not carried on a collision course with the exobase. Those ions that do strike the exobase in fact give rise to yet another loss process called sputtering. Therefore we briefly describe the plasma environment at Mars, and the interaction of the solar wind with a planetary atmosphere.

At Mars the plasma environment is determined by the solar wind (Figure 2), which consists of charged particles (mostly electrons and protons) and an embedded magnetic field. The solar wind originates in the solar corona and streams radially away from the Sun at high speeds (∼400 km/s). The solar wind proton density and temperature at Mars are $\sim 1 - 2\,\mathrm{cm}^{-3}$ and $\sim 4 \times 10^4\,\mathrm{K}$ [*Luhmann et al.*, 1992b]. The 25 day rotation period of the Sun causes the magnetic field lines (which are carried away from the Sun with the charged particles) to form a spiral shape with an increasing azimuthal component with heliocentric distance. At Mars, the magnetic field encounters the planet at an angle of ∼50 degrees, and has a magnitude of ∼3 nT [*Brain et al.*, 2003].

Planetary magnetospheres can be divided into three broad categories based on the obstacle that the planet presents to the solar wind. Earth and Jupiter present global obstacles to the solar wind by virtue of dynamo action in their electrically conducting and rotating interiors. Global magnetospheric obstacles rely mainly on the pressure of the global magnetic field ($B^2/2\mu_0$) to deflect the dynamic pressure of the solar wind (ρv^2). The Moon does not possess an intrinsic global magnetic field, and the solar wind plasma interacts directly with the planetary surface. Between these two extremes are planetary bodies like Venus and comets, which have no global magnetic field but do have atmospheres that are substantial enough to deflect the solar wind (Figure 3). In such an interaction solar radiation ionizes the upper portions of the atmosphere, creating an ionosphere. The flow of the solar wind particles past the planet leaves a wake region on the nightside where much of the solar wind plasma is excluded. The electrically conducting ionosphere interacts with the passing solar wind magnetic field, generating currents in the ionosphere that shield the lower portions of the atmosphere from the solar wind. The boundary at which this shielding occurs is usually called the ionopause, and is thought to be the location where the solar wind dynamic pressure is balanced by atmospheric pressure contributions, including ionospheric thermal pressure and magnetic pressure from ionospheric currents. This third type of magnetospheric obstacle is sometimes called an induced obstacle.

The question of which of the above categories Mars falls into has been the subject of some debate over the last 35 years. There were arguments for a magnetospheric obstacle [e.g. *Dolginov*, 1978a, b; *Dolginov et al.*, 1976], an ionospheric obstacle [e.g. *Russell et al.*, 1995; *Russell*, 1978a, b], a combined magnetospheric/ionospheric obstacle [e.g. *Bogdanov and Vaisberg*, 1975], and even a combined (ionospheric/remanent magnetism) obstacle [*Curtis and Ness*, 1988]. The most convincing evidence supported either an ionospheric or combined obstacle, and early observations detected a number of characteristic boundaries and plasma regions near Mars that had similarities to those observed at Venus and comets [see *Breus*, 1992]. Most recently, the MGS MAG/ER experiment resolved any lingering questions about the presence of a dynamo, reducing the upper limit on the Martian dipole moment by a factor of 5-10 compared to previous estimates, to $\sim 2 \times 10^{21}\,\mathrm{G-cm^3}$ [*Acuña et al.*, 1998]. To first order, then, Mars can be classified with Venus and comets as having an induced obstacle resulting from the interaction of the solar wind with an atmosphere. In the canonical solar wind / atmosphere interaction a number of boundaries are observed, including a bow shock upstream from the planet, a chemical boundary separating plasma dominated by solar wind protons from plasma significantly composed of planetary ions (called the cometopause, planetopause, Mass Loading Boundary, and Magnetic Pileup Boundary by different investigators), and a physical boundary called the ionopause, below which the solar wind is nominally excluded (analogous to a magnetopause at Earth). The solar wind magnetic field "drapes" around the atmospheric obstacle downstream from the shock on the planetary dayside. The tail region of Mars contains draped convected magnetic field lines.

Atmospheric Loss Processes

Atmospheric escape involves the loss of both neutral particles and ions from a planet. The known escape processes can be broadly classified according to whether they are primarily responsible for loss of neutrals or loss of ions, and according to whether they are important processes for the current Martian atmosphere (Table 1). Before an atmospheric particle can escape by any process, it must have an energy corresponding to a velocity in excess of the Martian escape velocity of $\sim$5 km/s. The escape energy for atomic hydrogen is about 0.1 eV, while an oxygen atom requires about 2 eV before it can escape.

Some escape processes contribute to atmospheric fractionation, where lighter species (or lighter isotopes of a single species) are preferentially removed, making the heavy species more abundant in the atmosphere. The most convincing observational evidence suggesting that the Martian atmosphere has been extensively depleted since its formation comes from measurements of a variety of isotopes, including hydrogen, carbon, nitrogen, argon, and xenon [*Jakosky and Jones*, 1997, and refs. therein]. Determination of the magnitude of atmospheric loss over Martian history is problematic for two reasons. First, the atmosphere has exchanged with different surface and subsurface reservoirs over its history, meaning that different amounts of atmospheric species have been available to the atmosphere at different epochs [*Jakosky and Jones*, 1997]. Second, processes other than escape (e.g. surface interactions) can contribute to fractionation [e.g. *Musselwhite and Drake*, 2000].

The main escape mechanisms are briefly summarized below

- **Hydrodynamic outflow** and impact erosion are not significant for the current atmosphere, but likely contributed to significant loss of neutrals early in Martian history. Hydrodynamic outflow occurs when a light species (such as hydrogen) is present in the upper atmosphere in abundance, with energy greater than the planetary escape velocity. The light species escapes to space, and drags heavier species along with it through collisions. Light species are prefentially carried away with the fluid outflow because gravity counter-acts the upward drag. This process is thought to be important for early terrestrial atmospheres, which were hydrogen rich [*Zahnle and Kasting*, 1986].

- **Impact erosion** removes atmospheric particles when the vapor plume from a large impactor (or the impactor itself for smaller objects) energizes and accelerates atmospheric particles above the escape velocity. This mechanism is most significant for large impactors, is assumed not to contribute to fractionation, and is a less species-selective process because of the manner in which the energy is deposited into the atmosphere. Impact erosion is thought to be the chief loss mechanism for Mars after hydrodynamic outflow ceased and before the end of the late heavy bombardment [*Melosh and Vickery*, 1989].

- **Thermal escape** occurs when a portion of the thermal distribution for an atmospheric species exceeds the energy necessary for escape. This process (also called Jeans escape) contributes to fractionation since lighter species require less energy to achieve escape velocity. Jeans escape is thought to be the dominant loss process for neutral atmospheric hydrogen at Mars [*Yung et al.*, 1988; *Kass*, 2001].

- **Non-thermal escape** is a collection of processes that result from additional energy inputs to certain atmospheric species. These processes include:
  - **Photochemical escape** In this process solar EUV radiation and ionospheric chemistry combine to produce a species that undergoes dissociative recombination. This reaction imparts superthermal energies to its atomic products, thereby increasing the fraction of atoms with energies above that needed for escape. This process is extremely important in the current Martian atmosphere [*Luhmann and Brace*, 1991], producing both direct escape of the key constituents O and N, and the hot oxygen corona that is a reservoir for the production of the pickup ions that escape and sputter neutrals as described below.
  - **Ion Pickup** The acceleration or pickup of atmospheric ions occurs because these charged particles experience an electric field from the magnetized solar wind when they are produced above the ionopause. They can be accelerated to speeds of up to 100s of km/s. Some are accelerated along trajectories that carry them downstream into the distant solar system, while others are on a collision course with the deeper atmosphere. The latter may participate in another nonthermal loss process called sputtering.
  - **Sputtering** is an escape process that can act to remove heavy atmospheric neutrals. Both solar wind protons and recently picked up ions impact the Martian atmosphere where they undergo charge exchange near the exobase. Charge exchange neutralizes the ion which then

imparts its relatively large energy to surrounding particles by collisions. If the collision products have upward velocities larger than the escape velocity they may be directly lost, while the rest contribute to the density of the neutral corona (which is the source of pickup ions in the first place, making an interesting feedback loop). The loss rate due to sputtering is debated in the literature [*Luhmann et al.*, 1992a; *Kass and Yung*, 1996]. It is thought to be a contributing loss process whose importance may have been especially significant early in Mars' history [*Luhmann et al.*, 1992a].

- **Bulk removal** of planetary atmospheres is thought to occur at Venus, Mars, and comets. These processes are not well-understood, and can include wave and fluid instabilities at the solar wind / atmosphere boundary layer that strip away large portions of the atmosphere at one time [*Perez-de-Tejada*, 1987], or outflows analogous to the Earth's "polar wind" [*Hartle and Grebowsky*, 1990].

Contemporary Processes

The loss mechanisms of Jeans escape, non-thermal chemical loss, ion pickup, and sputtering (listed above) are believed to be important for the current Martian atmosphere. Jeans escape is only thought to be relevant for atmospheric hydrogen [*Kass*, 2001]; the three latter processes are discussed here in further detail.

Mars' chief atmospheric constituent is CO_2[*Nier and McElroy*, 1977], and $O_2^+$is the dominant ionospheric ion [*Hanson et al.*, 1977] (Figure 4). While many atmospheric species escape, the relationship between the major loss processes can be illustrated by examining the possible fates of the oxygen that results from photolysis of CO_2(Figure 5). O_2^+formed by photolysis is a major constituent of the ionosphere. It dissociatively recombines to form hot oxygen atoms, some of which exceed the escape velocity and are lost from the atmosphere. Other hot oxygen atoms reach high altitudes, forming a corona. A fraction of these are ionized, and then picked up by the solar wind. Depending upon the orientation of the solar wind magnetic field with respect to Mars and the location of the oxygen when it is ionized, it is either lost by the pickup process, or re-impacts the planet. Re-impacting oxygen ions can cause multiple atmospheric atoms to be sputtered out of the atmosphere.

Evidence that the dissociative recombination process is active at Mars is inferred from ionospheric altitude profiles from the Viking landers (Figure 4), which showed that the Martian ionosphere is predominantly O_2^+ [*Hanson et al.*, 1977]. Dissociative recombination produces hot oxygen with a predicted energy distribution, part of which exceeds the escape velocity at Mars (Figure 6). In contrast, Venus has a CO_2 atmosphere and produces a hot oxygen corona, but the energy distribution of hot oxygen at Venus does not exceed the planetary escape speed. Dissociative recombination results in significant atmospheric loss at Mars of several important species; model calculations have been published for oxygen [*Fox and Hac*, 1997; *Kim et al.*, 1998; *Hodges Jr.*, 2000], nitrogen [*Fox*, 1993], and carbon [*Fox and Hac*, 1999; *Nagy et al.*, 2001].

Non-thermal photochemical processes supply the hot oxygen corona at Mars; solar wind pickup of ionized coronal atoms depletes it. As discussed above, pickup requires that atmospheric particles be ionized, and that they have access to the solar wind electric field. Three main ionization process act at Mars: photoionization, charge exchange, and electron impact ionization. The effects of each of these three ionization processes on pickup loss has been modeled, and all three are thought to be important [*Luhmann and Bauer*, 1992; *Zhang et al.*, 1993b; *Jin et al.*, 2001]. The solar wind is excluded below the ionopause, meaning that ions above the ionopause are subject to the pickup process. Indeed, photochemical models that do not include solar wind effects predict higher ionospheric densities than are actually observed at high altitudes (Figure 7), indicating that the solar wind is responsible for substantial removal of ions at the top [*Shinagawa and Cravens*, 1989]. The gyroradius of pickup ions at Mars can be large compared to the planetary radius, with the result that pickup is asymmetric with respect to the planet [*Wallis*, 1972]. Gyroradius scales with ion mass, and is inversely proportional to background field strength (gyroradii are not as large relative to the planetary radius at Earth or at Venus because the strength of the interplanetary field is lower at Mars, and because Mars is smaller). The gyroradius for O^+in a few nanotesla background magnetic field is several Mars radii. In the inner magnetosheath, where the draped interplanetary field is compressed against the obstacle to ~ 30 nT [*Vignes et al.*, 1998], the gyroradius is reduced to a fraction of a Mars radius. Sample pickup ion trajectories are shown for Venus and Mars in Figure 8. Pickup ions have been directly observed in the optical shadow of Mars by the ASPERA and TAUS instruments on the Phobos-2 spacecraft [*Lundin et al.*, 1990; *Verigin et al.*, 1992], as shown in Figure 9.

As mentioned above, not all pickup ions are expected to escape from Mars. The orientation of the solar wind magnetic field determines the path of a fresh pickup ion, and many of these new ions have trajectories that direct them down into the atmosphere as they are accelerated by the solar wind, as shown in Figure 9. Reimpacting oxygen ions can achieve energies as high as 10 keV (Figure 10). This energy is redistributed to neutral atmospheric particles below the exobase through charge exchange and other collisions, and some of these particles will be backscattered and escape. There is currently no observational proof that sputtering occurs at Mars. Observable evidence could consist of a coronal density that exceeds that expected for the photochemical source, or the direct detection of sputtered neutral particles.

Non-thermal mechanisms are more effective than Jeans escape at removing oxygen. However, Jeans escape can be an important loss process for hydrogen, which is sixteen times lighter than oxygen, and therefore has an escape energy which is sixteen times smaller. Hydrogen is lost in a variety of forms, including H, H2, D, and HD [*Yung et al.*, 1988]. Jeans escape is the dominant loss process for H [*Kass*, 2001], and dominates at solar maximum for H2 and D [*Krasnopolsky et al.*, 1998]. Non-thermal processes dominate the HD loss [*Kass*, 2001].

Other factors affecting the escape processes

A variety of other factors affect the above atmospheric escape processes at Mars. One extremely important parameter is the solar EUV radiation flux. Solar ionizing radiation has great influence over the ionosphere at Mars because it determines photoionization rates, and therefore affects the hot oxygen production and thus the amount of oxygen available for ionization and pickup by the solar wind. It also affects the rate of pickup ion production, and through the related sputtering, increases the coronal density in an interesting non-linear feedback loop. The solar EUV flux varies over timescales ranging from days to billions of years. In the current epoch, solar radiation is known to vary predictably over the solar cycle (Figure 11). The solar radio flux at 10.7 cm ($F_{10.7}$ is correlated with the sunspot number, and is commonly taken as a proxy for solar variability. The variation over the solar cycle is particularly large in the UV and EUV (Figure 12), which are the wavelengths that are important for photoionization. The amount of loss from Mars should be very different over the solar cycle; models predict factors of 10 or more difference between solar maximum and solar minimum [e.g. *Nagy et al.*, 2001; *Kim et al.*, 1998; *Fox*, 1997]. This is potentially important for understanding the evolutionary consequences, as will be discussed later, because the early Sun may have been bright in EUV wavelengths.

The solar wind also critically affects atmospheric loss. Variations in the the solar wind affect collison rates in the upper atmosphere, the strength of the IMF affects the gyroradii of pickup ions, and the solar wind dynamic pressure affects the altitude of the ionopause. While many models for present-day atmospheric loss explore the effects of changes in solar EUV on loss, very few consider only the effects of variations in the solar wind density, velocity, and magnetic field strength and orientation [*Luhmann et al.*, 1992a]. Finally, the solar wind not only removes atmospheric constituents, but may also serve as a source of volatiles (especially helium and rare gases) to the Martian atmosphere [e.g. *Krasnopolsky*, 2000].

Coronal Mass Ejections (CMEs) produce large ejections of coronal material into the solar wind that sometimes travel fast enough relative to the normal 400 km/s plasma flow to create an interplanetary shock wave. This shock wave produces large fluxes of energetic particles as well as a solar wind pressure pulse. A CME encounter with the Martian atmosphere could result in significant enhancement to the atmospheric escape flux for short periods of time if it leads to heating, extra ionization, or sputtering. The number and magnitude of CMEs encountering the Martian atmosphere may contribute substantially to time-averaged atmospheric loss rates. Analyses of this possible episodic increase of solar wind interaction losses remain to be done.

There is currently no evidence for a dynamo magnetic field at Mars, but regions of strongly magnetized crust have been observed by the Mars Global Surveyor MAG/ER instrument [*Acuña et al.*, 1998]. Crustal sources do not provide global atmospheric protection from solar wind scavenging. However, crustal sources may protect regions of atmosphere locally, forming "mini-magnetospheres" that provide sufficient magnetic pressure to deflect the solar wind to significant altitudes [*Acuña et al.*, 1999]. In addition, the field line configuration resulting from the interaction of the solar wind with crustal magnetic fields allows for unusual topologies where magnetic field lines connected at one end to the Martian surface can reconnect to the solar wind magnetic field, similar to the polar auroral regions at Earth [*Krymskii et al.*, 2002]. Such topologies would provide conduits for particle deposition into the Martian atmosphere (resulting in ionization and heating), and particle acceleration out of the ionosphere (escape). It is unclear whether this effect is significant at Mars.

Dust storms on Mars occur on an annual basis, and global, planet-encircling dust storms occur less frequently. Dust storms heat the atmosphere, and are known from radio occultation measurements to raise the ionosphere to higher altitudes as a result [*Zhang et al.*, 1990]. They also may affect the energetics and chemistry in the upper atmosphere, thereby affecting escape. The implications of these effects for loss rates are unknown.

Current Escape Rates

Investigators are reasonably certain that the major removal processes described above act at Mars, but there is disagreement about the present-day escape rates, and about the relative importance of these processes for different species. Three approaches have been employed to determine escape rates for neutrals and for ions: observation, basic estimates of total atmospheric loss rates, and models for individual species and/or processes.

Given the large number of spacecraft that have visited Mars relative to other solar system planets, it is suprising that there have not been more observations capable of addressing the problem of escape. As mentioned above, the Phobos spacecraft had two instruments that persistently measured heavy ions in the magnetotail of Mars. The ASPERA ion composition experiment had sufficient mass resolution to separate observed ions into three groups: H^+, O^+, and molecular ions [*Lundin et al.*, 1990]. Proton and heavy ion spectra were also measured by the TAUS spectrometer [*Verigin et al.*, 1992]. Outflowing ions were observed in the central tail, and also in the outer tail regions by both instruments, but there was disagreement about the magnitude of the ion fluxes, and the region of the tail where loss was greatest. In addition, TAUS estimates were based on ions with energy greater than 180 eV. Ion fluxes ranged from $\sim 10^6 - 10^7 \mathrm{cm}^{-2}\mathrm{s}^{-1}$. Translating fluxes into global loss rates requires an assumption about the area over which ionosphere is being lost, and the assumption that fluxes observed in the tail are characteristic of fluxes over the entire ionosphere. Overall, the estimated ion loss in the Martian tail was $\sim 10^{25}$ ions/s, or on the order of 1 kg/s of ionospheric loss.

Upper limits on global loss rates of ions may also be estimated using very simple physical considerations. In these rough estimates, the solar wind is assumed to transfer all of its momentum to stationary ionospheric ions, so that the mass flux of incident solar wind ions is equivalent to the mass flux of escaping planetary ions. The calculation is sensitive to assumptions about the cross-sectional area of the obstacle to the solar wind, which is probably quite variable. Different investigators have estimated upper limits of $\sim 4.5 \times 10^{25}$ions/s and $\sim 4 \times 10^{26}$ions/s, assuming that all escaping particles are atomic oxygen [*Luhmann and Bauer*, 1992; *Lundin et al.*, 1990]. Such calculations assume that the supply of ions to the ionosphere is rapid enough to maintain a steady state. A similar type of estimate is sometimes employed for individual species by using ionization rates of that species by different processes (electron impact, photoionization, and charge exchange), upper atmosphere neutral density profiles, and the assumption that all ions created above the ionopause will be lost (effectively ignoring re-impact and sputtering). This type of calculation predicts loss of $\sim 10^{25}$ ions/s, in general agreement with the loss rates inferred by the Phobos spacecraft [*Luhmann and Bauer*, 1992].

Physical models are a third commonly used means of prediction for atmospheric loss rates. A variety of models (and combinations of models) have been used, including Monte Carlo simulations [*Kallio and Barabash*, 2001; *Leblanc and Johnson*, 2001; *Jin et al.*, 2001; *Johnson et al.*, 2000; *Hodges Jr.*, 2000; *Kim et al.*, 1998; *Fox and Hac*, 1999; *Kass and Yung*, 1995, 1996], test particle models [*Cravens et al.*, 2002; *Leblanc and Johnson*, 2001; *Jin et al.*, 2001; *Kallio and Koskinen*, 1999; *Luhmann and Kozyra*, 1991], photochemical models [*Nair et al.*, 1994; *Krasnopolsky*, 1993; *Yung et al.*, 1988], MHD simulations [*Ma et al.*, 2002; *Liu et al.*, 2001], and two-stream models [*Nagy et al.*, 2001; *Nagy and Cravens*, 1988; *Kim et al.*, 1998]. These models have been applied to several mechanisms for many species, including (but not limited to) dissociative recombination of CO^+, O_2^+, and N_2^+ [*Hodges Jr.*, 2000; *Fox and Hac*, 1999, 1997; *Fox*, 1993; *Kim et al.*, 1998; *Nagy and Cravens*, 1988]; ionization and pickup of O and He [*Jin et al.*, 2001; *Kallio and Koskinen*, 1999; *Krasnopolsky and Gladstone*, 1996; *Krasnopolsky et al.*, 1993; *Luhmann and Kozyra*, 1991]; and sputtering of neutrals at the exobase by O^+pickup ions [*Johnson et al.*, 2000; *Hutchins and Jakosky*, 1996; *Kass and Yung*, 1995, 1996; *Luhmann and Kozyra*, 1991].

Each of the three approaches above has problems. Observations to date have not sampled loss from the entire atmosphere (Figure 13) and did not have the mass resolution required to determine loss rates for individual heavy ion species. Further, there have been no spacecraft measurements of neutral loss other than of hydrogen inferred from Lyman-alpha profiles measured by the Mariner spacecraft ultraviolet spectrometer. Estimates of total atmospheric loss are based on simplifying assumptions. Model-dependent predictions of atmospheric escape have become increasingly sophisticated. However, these models are poorly constrained by observations.

Table 2 summarizes the current escape rates due to processes unrelated to the solar wind for four biologically significant species: H, O, C, and N. The escape rates range from $10^{24}\mathrm{s}^{-1}$ to $10^{26}\mathrm{s}^{-1}$. Among these species, only H has been estimated entirely based on observations [*Krasnopolsky et al.*, 1998]. The escape rate for the other three species rely on model predictions, and have not been validated. Figure 14 suggests that the oxygen escape flux for Mars is comparable to the hydrogen escape flux at Earth in the form of polar wind and energetic neutral H from ring current decay.

Evolution of the Atmosphere

The relative importance of each process, and the escape rates for neutrals and ions has changed over Martian history. The history of the atmosphere as it is currently understood (cf. *Jakosky and Phillips* [2001]) is as follows: The original Martian atmosphere formed 4.6 Ga from impact delivery of volatiles and from outgassing events. Hydrodynamic escape stripped away the early atmosphere, until enough hydrogen had been removed that this fluid-like escape process was no longer possible. Impact erosion was the dominant escape process until the end of the late heavy bombardment (about 3.5 Ga), removing large portions of atmosphere with every large impact (but also adding volatiles to the atmosphere with every impact, large or small). A secondary atmosphere probably formed as a result of impact delivery and large outgassing events. A global magnetic field prevented escape by solar wind related mechanisms. After the flux of impactors declined, Jeans escape and photochemical mechanisms dominated neutral loss. After the dynamo ceased, solar-wind mechanisms dominated ion loss. These mechanisms have continued to remove and fractionate the atmosphere over the last 3.5–3.7 Gy. Exchanges with the polar caps and surface have also affected the atmosphere.

Three main factors have governed escape rates and the integrated atmospheric loss since the end of the late heavy bombardment. These are the timing of the Martian dynamo, the evolution of the solar ionizing radiation, and the evolution of the solar wind.

Current evidence supports the idea that Mars had a global dynamo early in its history and that this dynamo did not exist at the time of resurfacing of the northern hemisphere and at the time of formation of the two large southern impact craters (Hellas and Argyre) [*Acuña et al.*, 1999]. Recent experiments demonstrate that the oldest SNC meteorites formed in the presence of a strong magnetic field, and therefore the dynamo had turned on within the first 0.5 billion years of Martian history [*Weiss et al.*, 2000]. There is some debate as to whether the dynamo was capable of restarting later in Martian history [*Schubert et al.*, 2000]. A dynamo provides significant protection from solar wind related loss mechanisms (Figure 15), because the pickup process is only effective above the magnetopause. The altitude of the Martian magnetopause as a function of time is therefore an important parameter for evolutionary calculations, and the timing of the dynamo is an important constraint. Evolutionary calculations of atmospheric loss have incorporated different models for the time evolution of the global magnetic field (Figure 16), and for the altitude of the magnetopause (Figure 17). Additional atmospheric protection might be offered by crustal magnetic sources [*Acuña et al.*, 1999]. If these sources existed over the entire planet, and have gradually been erased by impacts and resurfacing events over Martian history, then solar wind mechanisms may have been largely prevented for a long period of time after the dynamo turned off [*Jakosky and Phillips*, 2001].

Observations of sun-type stars show that the solar EUV flux was substantially higher in the past than it is today (Figures 18) [*Ayres*, 1997]. Models predict that a higher EUV flux would account for higher exobase altitudes and increased scale heights (Figure 19), providing for the existence of ionosphere at higher altitudes than the present ionosphere, and a more extended corona (Figure 20). Both the dissociative recombination loss and the loss from pickup and sputtering would have been greater in the past as a result [*Luhmann et al.*, 1992a]. The magnitude of the solar cycle variability in EUV flux in the past is currently not known. Escape rates would have been affected if the solar activity level was higher.

Very little is known about the history of the solar wind, because observations of the solar wind at sun-type stars has to this point not been possible [*Ayres*, 1997]. Model predictions suggest that the flow velocity and field strength of the solar wind were higher in the past (Figure 21). A higher flow velocity would increase the incident mass flux at Mars (allowing for removal of a greater number of ions), as well as the dynamic pressure of the solar wind (reducing the altitude of the ionopause, above which pickup can occur). Higher field strength would decrease the gyroradii of pickup ions, perhaps affecting the fraction of pickup ions directly escaping versus participating in sputtering.

The integrated loss over Martian history is very difficult to determine. Models for ion production and sputtering loss have included the effects of EUV, solar wind, and possible dynamo models [*Hutchins et al.*, 1997; *Luhmann et al.*, 1992a]. It is generally predicted that loss rates were higher in the past than they are today [*Luhmann et al.*, 1992a; *Kass and Yung*, 1995, 1996]. Calculations that incorporate nominal EUV histories and solar wind behaviors estimate that the oxygen equivalent of a 50 m global water layer has been lost to space in the past 3.5 Gy, along with 150 mb of CO_2[*Luhmann et al.*, 1992a]. For comparison, the current atmosphere contains 6–7 mb CO_2, and has an atmospheric water content equivalent to a 7×10^{-6} m global layer. Other evolutionary models have accounted for 1 bar of atmospheric CO_2loss [*Kass and Yung*, 1995, 1996]. Isotope measurements seem to indicate that anywhere from $25 - 90\%$ of the atmosphere that existed at the last time that isotope ratios were "reset" has been removed through fractionating escape mechanisms [*Jakosky and Phillips*, 2001]. In addition, up to $50 - 90\%$ of the atmosphere that existed at the formation time of the oldest geologic surface units has been removed by impact erosion [*Brain and Jakosky*, 1998]. Overall, it is possible that substantial amounts of atmosphere have been removed in the last 3.5 Gy — perhaps enough to account for an early climate capable of supporting liquid water on the Martian surface.

Suggestions for Improved Understanding

Currently, our understanding of atmospheric escape at Mars is largely model-dependent, and is based on relatively few direct observations. Progress can be made in three general areas. First, the escape processes thought to remove atmosphere must be validated by observations. Second, observations should be made of global escape rates over time periods long enough to establish estimates of variability and the response to extreme conditions. Third, observations should be made that will improve models for the history of Martian atmospheric escape. Specific observations, model improvements, and spatial and time scales are discussed below.

Observations

Observations are vital to the improvement of estimates of current and past loss. Five observations are listed here, in order of priority:

- **Orbiting ion mass spectrometry** Ion mass spectrometers in orbit around Mars would both measure the lower altitude ($< 300\,\text{km}$) ionospheric cold ions that undergo dissociative recombination, thereby constraining the variability of the hot oxygen source, and at higher altitudes measure pickup ion fluxes moving down the wake and reimpacting the atmosphere. Special spectrometers would have to be developed to measure the low energy neutral sputtering products and validate the contribution of the sputtering process. Such spectrometers should improve on the mass resolution of the ASPERA instrument on Phobos 2, which was unable to distinguish between molecular ion species [*Lundin et al.*, 1990]. Several relevant instruments are on the Nozomi spacecraft, scheduled to arrive at Mars in 2004.

- **Ultraviolet spectrometry** A UVS instrument at Mars could provide much-needed information about energetic atmospheric neutrals in the corona. Its measurements could be used to infer the energy spectrum of neutrals produced by the dissociative recombination (and sputtering) process, as well as composition and density in the corona. In combination with the ionospheric ion measurements mentioned above, a UV instrument could establish some evidence for a sputtered component of the corona. Ultraviolet airglow emission at Mars between 1100 and 4000 $\mathring{A}$ was measured by the Mariner 6 and 7 spacecraft [*Barth et al.*, 1971], and includes emissions from CO, CO^+, CO_2^+, and O, as well as Lyman α. EUV measurements have been made of He at 584 $\mathring{A}$ [*Krasnopolsky et al.*, 1994]; O^+ and O^{++} emit in the EUV as well. Nozomi carries both EUV and FUV instruments.

- **Supporting EUV and Solar Wind measurements** Supporting measurements of the solar wind (velocity, density, and magnetic field) and solar EUV flux and energetic particles in concert with the above measurements are needed to understand the range of variability in escape over a solar cycle and under extreme solar activity conditions. In the absence of an upstream solar wind and EUV monitor at Mars, investigators are forced to make assumptions about the values of the relevant parameters. Many investigators adopt "typical" values of the relevant parameters, thereby assuming no time variability. Others [*Mitchell et al.*, 2000; *Vennerstrom et al.*, 2003] extrapolate from spacecraft measurements near Earth (these extrapolations are most reliable over long timescales).

- **Sun-like star observations** The history of the solar wind is poorly constrained from observations or models, and only the average history of the EUV flux for Sun-type stars is known. Observations of sun-type stars that provide information about the evolution of the solar wind, and information about the frequency and magnitude of variability in the EUV flux as a function of time would be useful for calculations of integrated loss at Mars. Recent models suggest achieving warmer temperatures on early Earth and Mars can be achieved by assuming that the early Sun was brighter than predicted by typical models; such a bright Sun might have existed if it were a few percent more massive than it is today [*Sackmann and Boothroyd*, 2003]. The assumptions of these models are testable using helioseismology [*Sackmann and Boothroyd*, 2003].

- **Low altitude field measurements** The chronology of the global field is important for evolutionary calculations of atmospheric loss. The timing of the Martian dynamo could be further constrained with low-altitude magnetic field surveys. These surveys would need to take place from an atmospheric platform, rather than from an orbiting spacecraft. The Mars Scout missions provide possible opportunities for this type of observation. Low altitude surveys are also of interest to investigators interested in looking for subsurface water on Mars on local scales [*Sprenke and Baker*, 2003].

Species and Scales

Different escaping species are important at Mars for different reasons. H,C,O, and N are biologically important species, and the rate at which they escape must be known before their current abundance in the atmosphere can be related to biological activity. In particular, their atmospheric abundance over Martian history gives clues to when biological processes were possible at Mars. The escape of H and O are especially important because they determine water loss at Mars, contribute to the oxidation state of the atmosphere and surface (is H escaping twice as fast as O?), and are important for the formation of many ancient and recent geologic features. C and O are important because $CO_2$is the chief atmospheric constituent, and a greenhouse gas that warmed the early atmosphere. The most likely explanation for the geologic evidence on Mars is that it had a thick CO_2atmosphere and a climate hospitable to liquid water long ago, and that much of the $CO_2$was lost. Lack of detection of abundant surface carbonates to this point [*Christensen et al.*, 1998] suggests that the $CO_2$was lost to space, but predictions for this loss vary by orders of magnitude. Integrated loss estimates for $CO_2$by all possible significant processes must be improved before we can reliably state what happened to the ancient atmosphere.

A variety of spatial domains are also important to measurements of present atmospheric escape. Ideally, a survey of escape at Mars would cover a wide range in altitude, solar zenith angle, and local time. In this way the uniformity (or nonuniformity) of the escape flux could be determined (Figure 13), including the low altitude photochemical processes and high altitude solar wind related processes. Simultaneous measurements by spacecraft in the equatorial plane and in a polar orbit would be tremendously useful, in addition to supporting solar EUV and solar wind measurements at Mars.

One key consideration for future measurement strategies is the timescale over which measurements are taken. For current escape rates, measurements should be taken over timescales ranging from one sol to one solar cycle. Crustal magnetic sources affect the ionopause altitude and the shape of the obstacle that Mars presents to the solar wind as Mars rotates. There may be seasonal or annual variation in escape due to dust storms or obliquity variation. The solar EUV flux varies periodically over the solar cycle, affecting ionization, ionopause altitudes, and escape. The effect of variations over each of these timescales must be considered when modeling the evolution of the Martian atmosphere.

Models

Improved models will result from improved observations. Model refinements will have the largest impact in the area of atmospheric evolution. First, models of the early Martian atmosphere are needed to provide initial conditions for calculations of integrated loss over Martian history. Models of the early EUV flux already exist, but the variability superposed on the "average" EUV history has not been determined. There are very few models of the history of the solar wind, which is responsible for pickup and sputtering loss. Finally, a time history of the Martian global magnetic field is critical for determining the extent to which the solar wind related loss processes which are important today acted in the past.

Astrobiological Implications

The discussions above focus on the current understanding of atmospheric escape at Mars, and suggested measurements for an improved understanding and extrapolation to the past. The astrobiological connections of the proposed measurements are less direct. Martian biology would have to measurably affect the species or processes involved, either in the ionosphere, in the exosphere, or at the exobase. In this case, study of the lower atmosphere would be a more direct method of detecting these anomalies, and would further enable the detection of "local" atmospheric biosignatures confined to limited geographic regions.

Isotope ratios are commonly taken as proof that escape has occurred at Mars, with heavier isotopes more abundant than light isotopes. If there were an isotope ratio that could be affected by biology, did not fit the observed trend in isotope ratios of different species (e.g. favored the light isotope), and could not be explained by escape or geological processes, then one might consider biological activity as a potential contributor. However, given the probability that different resevoirs have been in contact with the Martian atmosphere at different times over its history, unambiguous interpretation of a biological isotopic signature seems unlikely.

Another possible biosignature could be present in the oxidation state of the Martian atmosphere. For example, if Mars is observed to have an oxidizing atmosphere, but escape and other loss processes cannot account for sufficient loss of reducing species, then biology might be at work.

Each of the above approaches contains uncertainties that may never be resolved. Perhaps the most promising constraint that studies of atmospheric escape can place on Martian biological activity is not in the area of biosignature detection, but in determination of the climate and atmospheric composition at each point in Martian history. If we could state with reasonable certainty what elements and climate conditions would have been available to life on Mars as a function of time, then we could say something about when and where life might have existed on Mars, and where evidence of that life might be preserved today.

Acknowledgements

This paper is based on a presentation by J. Luhmann at the Mars Atmospheric Chemistry and Astrobiology Workshop in Pasadena, Calfornia in December of 2001.

References

Acuña, M., et al., Magnetic field and plasma observations at Mars: Initial results of the Mars Global Surveyor mission, *Science*, *279*, 1676–1670, 1998.

Acuña, M., et al., Global distribution of crustal magnetization discovered by the Mars Global Surveyor MAG/ER experiment, *Science*, *284*, 790–793, 1999.

Ayres, T., Evolution of the solar ionizing flux, *J. Geophys. Res.*, *102*, 1641–1651, 1997.

Barth, C., C. Hord, J. Pearce, K. Kelly, G. Anderson, and A. Stewart, Mariner-6 and Mariner-7 ultraviolet spectrometer experiment - Upper atmosphere data, *J. Geophys. Res.*, *76*, 2213–2227, 1971.

Bogdanov, A., and O. Vaisberg, Structure and variations of solar wind-Mars interaction region, *J. Geophys. Res.*, *80*, 480, 1975.

Brain, D., and B. Jakosky, Atmospheric loss since the onset of the Martian geologic record: Combined role of impact erosion and sputtering, *J. Geophys. Res.*, *103*, 22,689–22,694, 1998.

Brain, D., F. Bagenal, M. Acuña, and J. Connerney, Martian magnetic morphology: Contributions from the solar wind and crust, *J. Geophys. Res.*, 2003.

Breus, T., *Venus and Mars: Atmospheres, ionospheres, and solar wind interactions*, vol. 66 of *Geophysical Monograph*, chap. The solar wind interaction with Mars over the solar cycle: A post-Phobos view, pp. 387–403, American Geophysical Union, 1992.

Christensen, P., et al., Mars Global Surveyor Thermal Emission Spectrometer experiment: Investigation description and surface science results, *Geophys. Res. Lett.*, *25*, 2753–2756, 1998.

Cravens, T., A. Hoppe, S. Ledvina, and S. McKenna-Lawlor, Pickup ions near Mars associated with escaping oxygen atoms, *J. Geophys. Res.*, *107*, 7–1 – 7–9, 2002.

Curtis, B., and N. Ness, The global magnetic field of Mars and implications for crustal evolution, *Geophys. Res. Lett.*, *15*, 737–739, 1988.

Des Marais, D., et al., Remote sensing of planetary properties and biosignatures on extrasolar terrestrial planets, *Astrobiology*, *2*, 153–181, 2002.

Dolginov, S., On the magnetic field of Mars - Mars 5 evidence, *Geophys. Res. Lett.*, *5*, 93–95, 1978a.

Dolginov, S., On the magnetic field of Mars - Mars 2 and 3 evidence, *Geophys. Res. Lett.*, *5*, 89–92, 1978b.

Dolginov, S., Y. Yeroshenko, and L. Zhuzgov, The magnetic field of Mars according to the data from the Mars 3 and Mars 5, *J. Geophys. Res.*, *81*, 3353–3362, 1976.

Donahue, T., J. Hoffman, R. Hodges, Jr., and A. Watson, Venus was wet: A measurement of the ratio of deuterium to hydrogen, *Science*, *216*, 630–633, 1982.

Fox, J., The production and escape of nitrogen atoms on Mars, *J. Geophys. Res.*, *98*, 3297–3310, 1993.

Fox, J., Upper limits to the outflow of ions at Mars: Implications for atmospheric evolution, *Geophys. Res. Lett.*, *20*, 1747–1750, 1997.

Fox, J., and A. Hac, Spectrum of hot O at the exobases of the terrestrial planets, *J. Geophys. Res.*, *102*, 24,005–24,011, 1997.

Fox, J., and A. Hac, Velocity distributions of C atoms in CO^+ dissociative recombination: Implications for photochemical escape of C from Mars, *J. Geophys. Res.*, *104*, 24,729–24,737, 1999.

Hanson, W., S. Santani, and D. Zuccaro, The Martian ionosphere as observed by the viking retarding potential analyzers, *J. Geophys. Res.*, *82*, 4351–4363, 1977.

Hartle, R., and J. Grebowsky, Upward ion flow in ionospheric holes on Venus, *J. Geophys. Res.*, *95*, 31, 1990.

Hodges Jr., R. R., Distributions of hot oxygen for Venus and Mars, *J. Geophys. Res.*, *105*, 6971–6981, 2000.

Hutchins, K., and B. Jakosky, Evolution of Martian atmospheric argon: Implications for sources of volatiles, *J. Geophys. Res.*, *101*, 14,933–14,949, 1996.

Hutchins, K., B. Jakosky, and J. Luhmann, Impact of a paleomagnetic field on sputtering loss of Martian atmospheric argon and neon, *J. Geophys. Res.*, *102*, 9183–9189, 1997.

Jakosky, B., and R. Haberle, *Mars*, chap. The seasonal behavior of water on Mars, pp. 969–1016, Univ. Arizona Press, Tucson, 1992.

Jakosky, B., and J. Jones, The history of Martian volatiles, *Reviews of Geophysics*, *35*, 1–16, 1997.

Jakosky, B., and R. Phillips, Mars volatile and climate history, *Nature*, *412*, 237–244, 2001.

Jin, H., T. Mukai, , T. Tanaka, and K. Maezawa, Oxygen ions escaping from the dayside Martian upper atmosphere, *Adv. Space Res.*, *27*, 1825–1830, 2001.

Johnson, R., D. Schnellenberger, and M. Wong, The sputtering of an oxygen thermosphere by energetic O^+, *J. Geophys. Res.*, *105*, 1659–1670, 2000.

Kallio, E., and S. Barabash, Atmospheric effects of precipitating energetic hydrogen atoms on the Martian atmosphere, *J. Geophys. Res.*, *106*, 165–177, 2001.

Kallio, E., and H. Koskinen, A test particle simulation of the motion of oxygen ions and solar wind protons near Mars, *J. Geophys. Res.*, *104*, 557–579, 1999.

Kallio, E., H. Koskinen, S. Barabash, C. Nairn, and K. Schwingenschuh, Oxygen outflow in the Martian magnetotail, *Geophys. Res. Lett.*, *22*, 2449–2452, 1995.

Kass, D., Loss of water to space from Mars: Processes and implications, in *American Geophysical Union, Fall Meeting 2001, abstract #P12E-02*, 2001.

Kass, D., and Y. Yung, Loss of atmosphere from Mars due to solar wind-induced sputtering, *Science*, *268*, 697–699, 1995.

Kass, D., and Y. Yung, Loss of atmosphere from Mars: Response, *Science*, *274*, 1932–1933, 1996.

Kim, J., A. Nagy, J. Fox, and T. Cravens, Solar cycle variability of hot oxygen atoms at Mars, *J. Geophys. Res.*, *103*, 29,339–29,342, 1998.

Krasnopolsky, V., Solar cycle variations of the hydrogen escape rate and the CO mixing ratio on Mars, *Icarus*, *101*, 33–41, 1993.

Krasnopolsky, V., On the Deuterium abundance on Mars and some related problems, *Icarus*, *148*, 597–602, 2000.

Krasnopolsky, V., and G. Gladstone, Helium on Mars: EUVE and PHOBOS data and implications, *J. Geophys. Res.*, *101*, 15,765–15,772, 1996.

Krasnopolsky, V., S. Chakrabarti, and G. Gladstone, Helium in the Martian atmosphere, *J. Geophys. Res.*, *98*, 15,061–15,068, 1993.

Krasnopolsky, V., S. Bowyer, S. Chakrabarti, G. Gladstone, and J. McDonald, First measurement of helium on Mars: Implications for the problem of radiogenic gases on the terrestrial planets, *Icarus*, *109*, 337–351, 1994.

Krasnopolsky, V., M. Mumma, and G. Gladstone, Detection of atomic deuterium in the upper atmosphere of Mars, *Science*, *280*, 1576–1580, 1998.

Krymskii, A., T. Breus, M. Acuña, J. Connerney, D. Crider, D. Mitchell, and S. Bauer, Structure of the magnetic field fluxes connected with crustal magnetization and top-side ionosphere at Mars, *J. Geophys. Res.*, 2002.

Leblanc, F., and R. Johnson, Sputtering of the Martian atmosphere by solar wind pick-up ions, *Planet Space Sci.*, *49*, 645–656, 2001.

Lederberg, J., Signs of life: Criterion-system of exobiology, *Nature*, *207*, 9–13, 1965.

Liu, Y., A. Nagy, T. Gombosi, D. DeZeeuw, and K. Powell, The solar wind interaction with Mars: Results of three-dimensional three-species MHD studies, *Adv. Space Res.*, *27*, 1837–1846, 2001.

Lovelock, J., A physical basis for life detection experiments, *Nature*, *207*, 568–570, 1965.

Luhmann, J., A model of the ion wake of Mars, *Geophys. Res. Lett.*, *17*, 869–872, 1990.

Luhmann, J., *Introduction to Space Physics*, chap. Plasma Interactions with Unmagnetized Bodies, pp. 203–226, Cambridge University Press, 1995.

Luhmann, J., and S. Bauer, *Venus and Mars: Atmospheres, ionospheres, and solar wind interactions*, vol. 66 of *Geophysical Monograph*, chap. Solar wind effects on atmosphere evolution at Venus and Mars, pp. 417–430, American Geophysical Union, 1992.

Luhmann, J., and L. Brace, Near-Mars space, *Rev. Geophys.*, *29*, 121–140, 1991.

Luhmann, J., and J. Kozyra, Dayside pickup oxygen ion precipitation at Venus and Mars: Spatial distributions, energy deposition and consequences, *J. Geophys. Res.*, *96*, 5457–5467, 1991.

Luhmann, J., R. Johnson, and M. Zhang, Evolutionary impact of sputtering of the Martian atmosphere by O^+ pickup ions, *Geophys. Res. Lett.*, *19*, 2151–2154, 1992a.

Luhmann, J., C. Russell, L. Brace, and O. Vaisberg, *Mars*, chap. The intrinsic magnetic field and solar-wind interaction of Mars, pp. 1090–1134, Univ. Arizona Press, Tucson, 1992b.

Lundin, R., A. Zakharov, R. Pellinen, H. Borg, E. Dubinin, B. Hultqvist, H. Koskinen, I. Liede, and N. Pissarenko, ASPERA/Phobos measurements of the ion outflow from the Martian ionosphere, *Geophys. Res. Lett.*, *17*, 873–876, 1990.

Ma, Y. A. N., K. Hansen, D. DeZeeuw, T. Gombosi, and K. Powell, Three-dimensional multispecies MHD studies of the solar wind interaction with Mars in the presence of crustal fields, *J. Geophys. Res.*, *107*, 6–1, 2002.

Melosh, H., and A. Vickery, Impact erosion of the primordial atmosphere of Mars, *Nature*, *338*, 487–489, 1989.

Michel, F., Solar-wind induced mass loss from magnetic field-free planets, *Planet Space Sci.*, *19*, 1583–1585, 1971.

Mitchell, D., R. Lin, H. Rème, D. Crider, P. Cloutier, J. Connerney, M. Acuña, and N. Ness, Oxygen Auger electrons observed in Mars' ionosphere, *Geophys. Res. Lett.*, *27*, 1871–1874, 2000.

Mitchell, D., R. Lin, C. Mazelle, H. Rème, P. Cloutier, J. connerney, M. Acuña, and N. Ness, Probing Mars' crustal magnetic field and ionosphere with the MGS Electron Reflectometer, *J. Geophys. Res.*, *106*, 23,419–23,427, 2001.

Musselwhite, D., and M. Drake, Early outgassing of Mars: Implications from experimentally determined solubility of iodine in silicate magmas, *Icarus*, *148*, 160–175, 2000.

Nagy, A., and T. Cravens, Hot oxygen atoms in the upper atmospheres of Venus and Mars, *Geophys. Res. Lett.*, *15*, 433–435, 1988.

Nagy, A., M. Liemohn, J. Fox, and J. Kim, Hot carbon densities in the exosphere of Mars, *J. Geophys. Res.*, *106*, 21,565–21,568, 2001.

Nair, H., M. Allen, A. Anbar, Y. Yung, and R. Clancy, A photochemical model of the Martian atmosphere, *Icarus*, *111*, 124–150, 1994.

Newkirk Jr., G., Solar variability on time scales of 10^5 years to $10^{9.6}$ years, in *The Ancient Sun*, edited by R. Pepin, J. Eddy, and R. Merrill, vol. 13 of *Geochemica et Cosmo de chemica Acta Suppl.*, p. 293, Pergamon Press, 1980.

Nier, A., and M. McElroy, Composition and structure of Mars' upper atmosphere: results from the neutral mass spectrometers on Viking 1 and 2, *J. Geophys. Res.*, *82*, 4341–4349, 1977.

Perez-de-Tejada, H., Plasma flow in the Mars magnetosphere, *J. Geophys. Res.*, *92*, 4713, 1987.

Pollack, J., Climatic change on the terrestrial planets, *Icarus*, *37*, 479–553, 1979.

Russell, C., The magnetic field of Mars: Mars 3 evidence reexamined, *Geophys. Res. Lett.*, *5*, 81–84, 1978a.

Russell, C., The magnetic field of Mars: Mars 5 evidence re-examined, *Geophys. Res. Lett.*, *5*, 85–88, 1978b.

Russell, C., T. Mulligan, M. Delva, T. Zhang, and K. Schwingenschuh, A simple test of the induced nature of the Martian tail, *Planet Space Sci.*, *43*, 875–879, 1995.

Sackmann, I.-J., and A. Boothroyd, Our Sun. V. A bright young Sun consistent with helioseismology and warm temperatures on ancient Earth and Mars, *Astrophys. J.*, *583*, 1024–1039, 2003.

Sagan, C., W. Thompson, R. Carlson, D. Gurnett, and C. Hord, A search for life on Earth from the Galileo spacecraft, *Science*, *365*, 715–721, 1993.

Schubert, G., C. Russell, and W. Moore, Timing of the Martian dynamo, *Nature*, *408*, 666–667, 2000.

Shinagawa, H., and T. Cravens, A one-dimensional multispecies magnetohydrodynamic model of the dayside ionosphere of Mars, *J. Geophys. Res.*, *94*, 6506–6516, 1989.

Sprenke, K., and L. Baker, Exploring for water on Mars: The case for mapping the low altitude magnetic field, *J. Geophys. Res.*, *108*, 6–1, 2003.

Summers, M. E., B. J. Lieb, E. Chapman, and Y. L. Yung, Atmospheric biomarkers of subsurface life on Mars, *Geophys. Res. Lett.*, *29*, 24–1, 2002.

Vennerstrom, S., N. Olsen, M. Purucker, M. A. na, and J. Cain, The magnetic field in the pile-up region at Mars, and its variation with the solar wind, *Geophys. Res. Lett.*, *30*, 22–1, 2003.

Verigin, M., et al., The Martian atmosphere dissipation problem: Phobos-2 TAUS experiment evidences, *Adv. Space Res.*, *12*, 23–26, 1992.

Vignes, D., C. Mazelle, and H. Rème, Preliminary study of crustal magnetic field in Acidalia Planitia, 1998, toulouse meeting.

Wallis, M., Comet-like interaction of Venus with the solar wind I, *Cosmic Electrodyn.*, *3*, 45, 1972.

Wayne, R., Atmospheric chemistry: the evolution of our atmosphere, *J. Photochem. Photobiol. A: Chem.*, *62*, 379–396, 1992.

Weiss, B., J. Kirschvink, F. Baudenbacher, H. Vali, N. Peters, F. Macdonald, and J. Wikswo, A low temperature transfer of ALH84001 from Mars to Earth, *Science*, *290*, 791–795, 2000.

Yung, Y., J.-S. Wen, J. Pinto, M. Allen, K. Pierce, and S. Paulson, Hdo in the Martian atmosphere: Implications for the abundance of crustal water, *Icarus*, *76*, 146–159, 1988.

Zahnle, K., and J. Kasting, Mass fractionation during transonic escape and implications for loss of water from Mars and Venus, *Icarus*, *68*, 462–480, 1986.

Zhang, M., J. Luhmann, A. Kliore, and J. Kim, A post-pioneer Venus reassessment of the Martian dayside ionosphere as observed by radio occultation methods, *J. Geophys. Res.*, *95*, 14,829–14,839, 1990.

Zhang, M., J. Luhmann, S. Bougher, and A. Nagy, The ancient oxygen exosphere of mars: Implications for atmospheric evolution, *J. Geophys. Res.*, *98*, 10,915–10,923, 1993a.

Zhang, M., J. Luhmann, A. Nagy, J. Spreiter, and S. Stahara, Oxygen ionization rates at Mars and Venus: Relative contribution of impact ionization and charge exchange, *J. Geophys. Res.*, *98*, 3311–3318, 1993b.

Figure 1. Cartoon of possible atmospheric sources and sinks for Mars.

Figure 2. Diagram showing radial solar wind plasma outflow with embedded magnetic field lines, and the interaction of the solar wind with a planetary obstacle.

Figure 3. Interaction of the solar wind with a planetary atmosphere. From *Luhmann* [1995].

Figure 4. Viking altitude profiles of the neutral Martian atmosphere [*Nier and McElroy*, 1977], and the ionosphere [*Hanson et al.*, 1977].

Figure 5. Possible avenues of loss for atmospheric oxygen.

Figure 6. Expected energy distributions for hot oxygen at Venus (top) and Mars (bottom). From [*Luhmann and Kozyra*, 1991].

Figure 7. Comparison of a model prediction for ionospheric density in the absence of any magnetic fields (top) to actual ionospheric density altitude profiles (bottom). From *Shinagawa and Cravens* [1989].

Figure 8. Test particle trajectories for O^+at Venus (top), O^+at Mars (middle). From *Luhmann* [1990].

Figure 9. (top) Cartoon of the solar wind interaction with Mars. Atmospheric ions accelerated by the solar wind are either carried downstream, or re-impact the atmosphere. From *Luhmann* [1995]. (bottom) Locations of oxygen ions ob-

served downstream from Mars by ASPERA, from *Kallio et al.* [1995]. Locations are projected into the y-z plane (in aberrated coordinates). Low energy oxygen is observed in the central tail region, while high energy oxygen is observed in the outer tail.

Figure 10. Energy spectra of precipitating O^+ions for Venus and Mars, calculated from a test particle model. From *Luhmann and Kozyra* [1991].

Figure 11. Correlation of sunspot number (a) and flux at 10.7 cm (b) over 5 solar cycles.

Figure 12. Solar irradiance as a function of wavelength (a), and the variability over a single solar cycle (b). The variability is particularly large in the UV and EUV.

Figure 13. Cartoon diagram showing the uncertainty in the determination of the flux of escaping ions at Mars. Neither the spatial extent over which escaping ions can be observed nor the spatial uniformity of the escape flux have not been measured.

Figure 14. Planetary source strengths of different elements to the solar wind as a function of heliocentric distance.

Figure 15. Comparison of the spatial extent of the Martian solar wind interaction to that at Earth. From *Luhmann and Brace* [1991].

Figure 16. Two models for the time evolution of the Martian dynamo, based on the sulfur content of the core. From *Hutchins et al.* [1997].

Figure 17. Magnetopause altitude above the subsolar point calculated for the model with xs=0.14 from Figure 16. From *Hutchins et al.* [1997].

Figure 18. Predicted time evolution of solar EUV luminosity (bottom), in units of the contemporary value.

Figure 19. Atmospheric profiles for O and $CO_2$for different values of the solar EUV flux. The exobase altitude was higher in the past. From a model calculation by *Luhmann et al.* [1992a].

Figure 20. Model hot oxygen density profiles for different values of the solar EUV flux. From *Luhmann et al.* [1992a] and *Zhang et al.* [1993a].

Figure 21. Modeled time evolution of the solar wind velocity and magnetic field strength, adapted from *Newkirk Jr.* [1980] by *Zhang et al.* [1993a] and *Luhmann et al.* [1992a].

Table 1 Mechanisms for Loss to Space

NEUTRALS	IONS
hydrodynamic outflow	ion pickup
impact erosion	bulk removal
thermal escape	
photochemical escape	
sputtering	

Table 2 Non-Solar Wind Related Current Escape Rates (Global atoms/s)

H	1.2×10^{26}	measurements[a]
O	$.5 \times 10^{25} - 1 \times 10^{25}$	measurements[b] and models[c]
C	$2 \times 10^{24} - 1 \times 10^{25}$	model[d]
N	3×10^{26}	model[c]

[a]Ly α corona
[b]Viking ionosphere
[c]dissociative recombination
[d]photodissociation

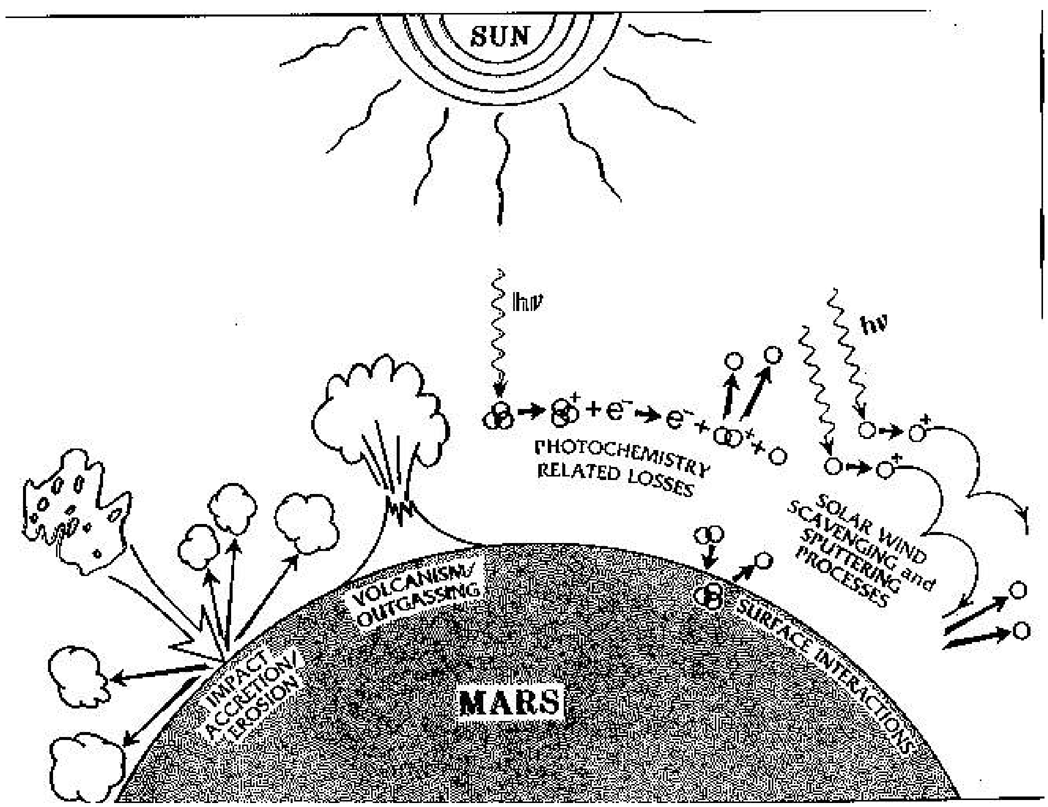
SUN
hν
hν
PHOTOCHEMISTRY
RELATED LOSSES
SOLAR WIND
SCAVENGING and
SPUTTERING
PROCESSES
IMPACT
ACCRETION/
EROSION
VOLCANISM/
OUTGASSING
SURFACE INTERACTIONS
MARS

Figure 1

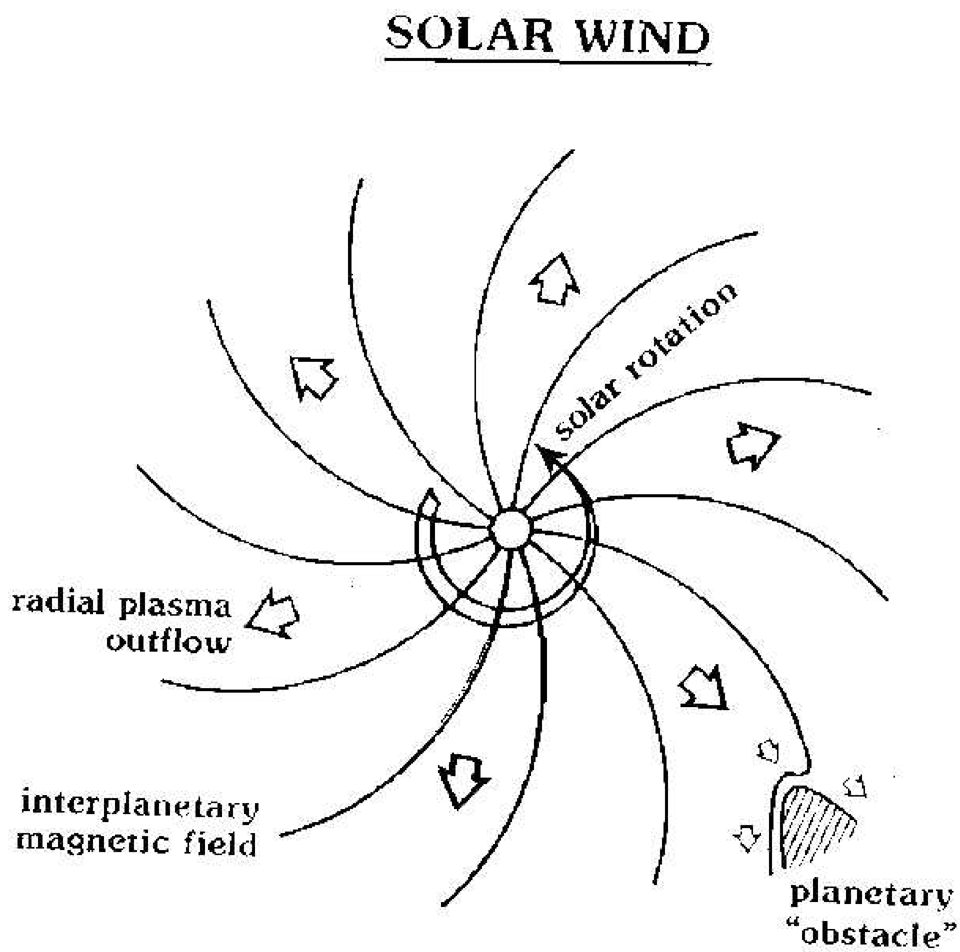
SOLAR WIND
solar rotation
radial plasma
outflow
interplanetary
magnetic field
planetary
"obstacle"

Figure 2

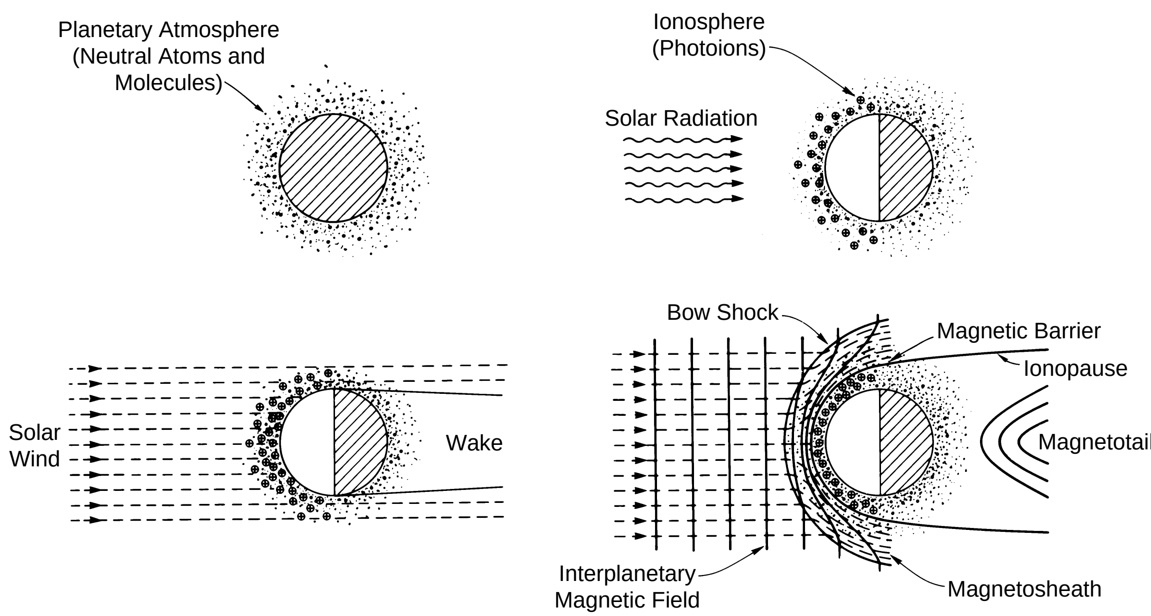
Planetary Atmosphere
(Neutral Atoms and
Molecules)
Ionosphere
(Photoions)
Solar Radiation
Solar
Wind
Wake
Bow Shock
Magnetic Barrier
Ionopause
Magnetotail
Interplanetary
Magnetic Field
Magnetosheath

Figure 3

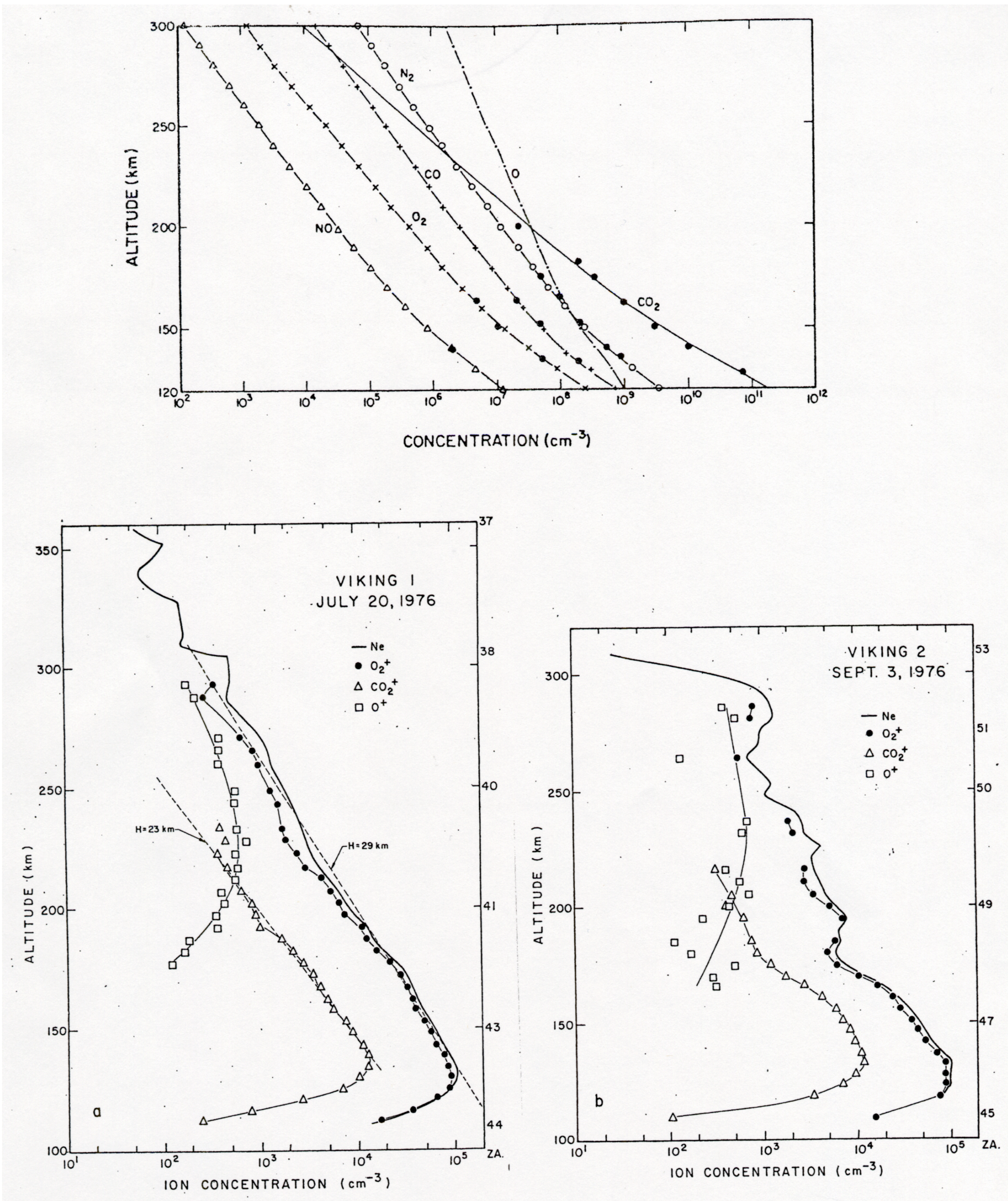

ALTITUDE (km)
CONCENTRATION (cm^{-3})
N_2
CO
O
O_2
NO
CO_2
VIKING 1
JULY 20, 1976
Ne
O_2^+
CO_2^+
O^+
H=23 km
H=29 km
a
ALTITUDE (km)
ION CONCENTRATION (cm^{-3})
ZA.
VIKING 2
SEPT. 3, 1976
Ne
O_2^+
CO_2^+
O^+
b
ALTITUDE (km)
ION CONCENTRATION (cm^{-3})
ZA.

Figure 4

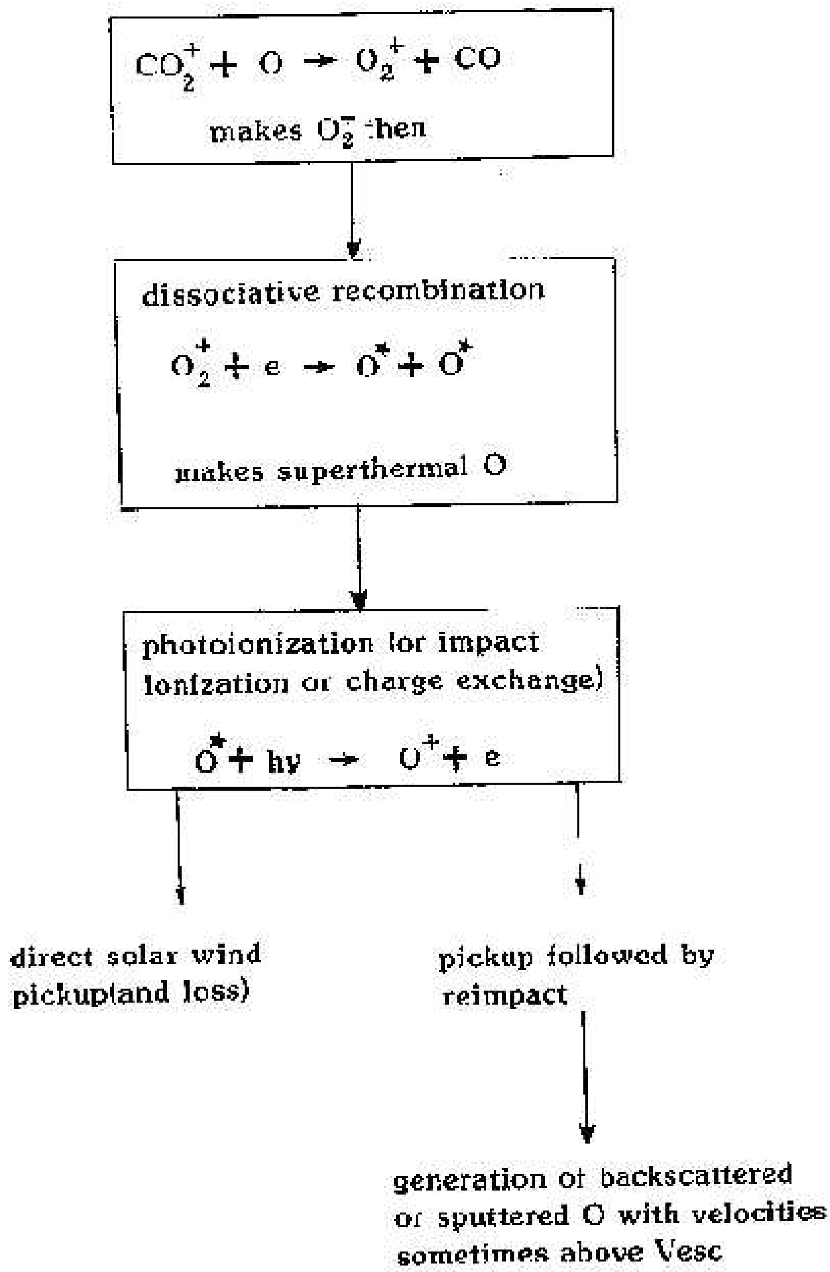

CO2+ + O → O2+ + CO
makes O2+ then
dissociative recombination
O2+ + e → O* + O*
makes superthermal O
photoionization (or impact ionization or charge exchange)
O* + hν → O+ + e
direct solar wind pickup(and loss)
pickup followed by reimpact
generation of backscattered or sputtered O with velocities sometimes above Vesc

Figure 5

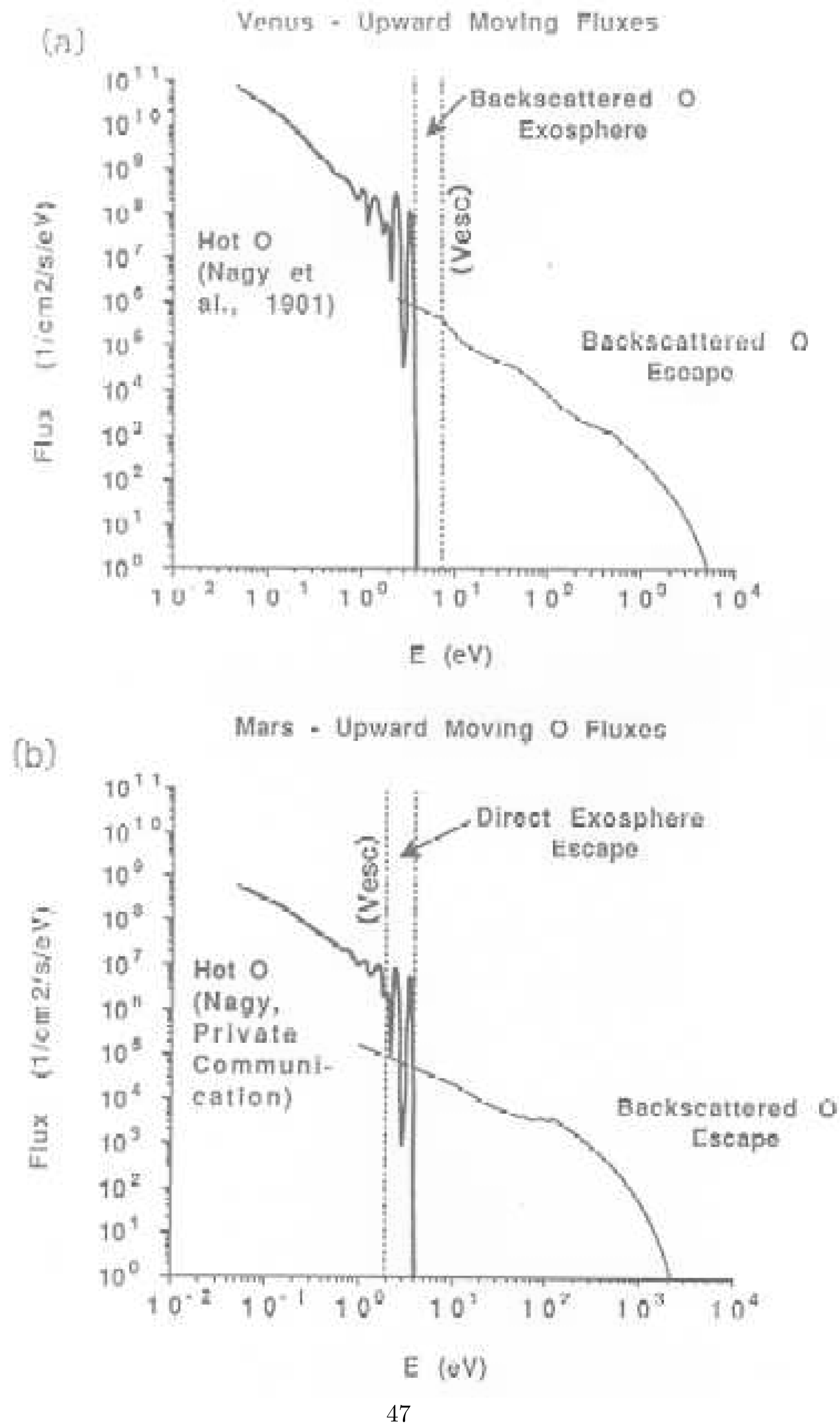

Venus - Upward Moving Fluxes
(a)
Backscattered O
Exosphere
(Vesc)
Hot O
(Nagy et
al., 1901)
Backscattered O
Escape
Flux (1/cm2/s/eV)
E (eV)
Mars - Upward Moving O Fluxes
(b)
Direct Exosphere
Escape
(Vesc)
Hot O
(Nagy,
Private
Communi-
cation)
Backscattered O
Escape
Flux (1/cm2/s/eV)
E (eV)

Figure 6

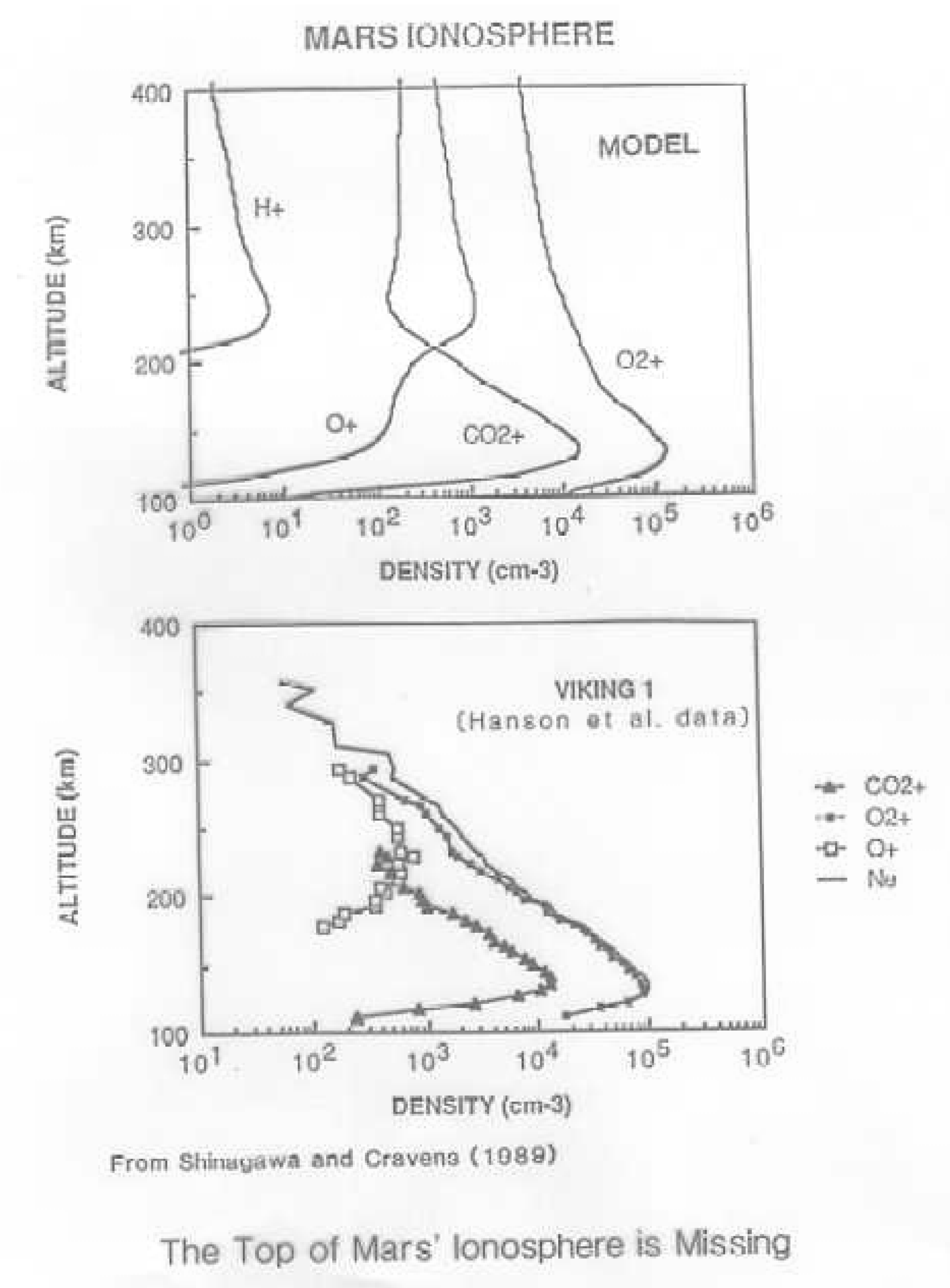
MARS IONOSPHERE
MODEL
H+
O+
CO2+
O2+
ALTITUDE (km)
DENSITY (cm-3)
VIKING 1
(Hanson et al. data)
CO2+
O2+
O+
Ne
From Shinagawa and Cravens (1989)
The Top of Mars' Ionosphere is Missing

Figure 7

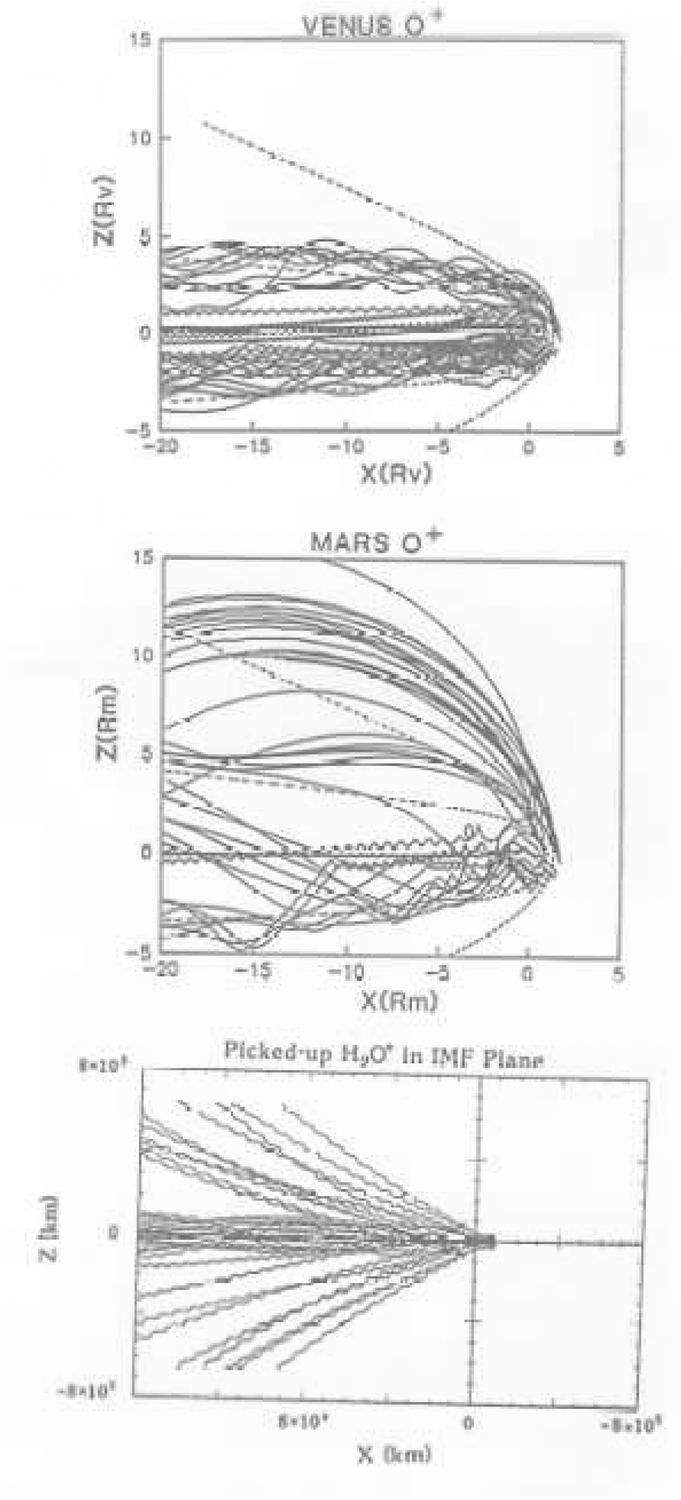
VENUS O+
Z(Rv)
X(Rv)
MARS O+
Z(Rm)
X(Rm)
Picked-up H2O+ in IMF Plane
Z (km)
X (km)

Figure 8

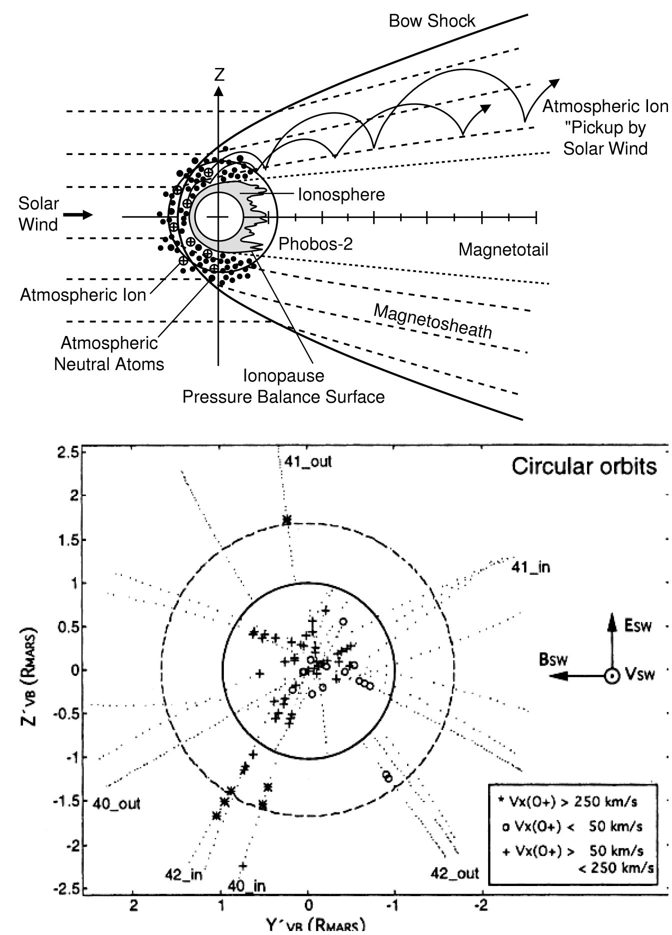
Bow Shock
Z
Atmospheric Ion
"Pickup by
Solar Wind
Ionosphere
Solar
Wind
Phobos-2
Magnetotail
Atmospheric Ion
Magnetosheath
Atmospheric
Neutral Atoms
Ionopause
Pressure Balance Surface
Circular orbits
41_out
41_in
40_out
42_in
40_in
42_out
ESW
BSW
VSW
* Vx(O+) > 250 km/s
o Vx(O+) < 50 km/s
+ Vx(O+) > 50 km/s
< 250 km/s
Z´VB (RMARS)
Y´VB (RMARS)

Figure 9

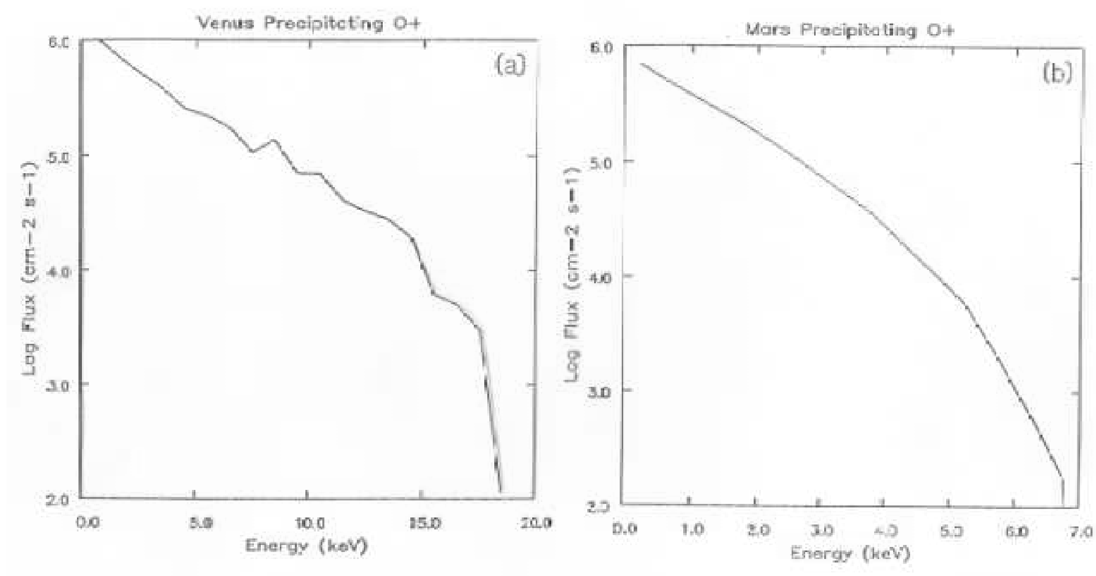
Venus Precipitating O+
(a)
Log Flux (cm−2 s−1)
6.0
5.0
4.0
3.0
2.0
0.0
5.0
10.0
15.0
20.0
Energy (keV)
Mars Precipitating O+
(b)
Log Flux (cm−2 s−1)
6.0
5.0
4.0
3.0
2.0
0.0
1.0
2.0
3.0
4.0
5.0
6.0
7.0
Energy (keV)

Figure 10

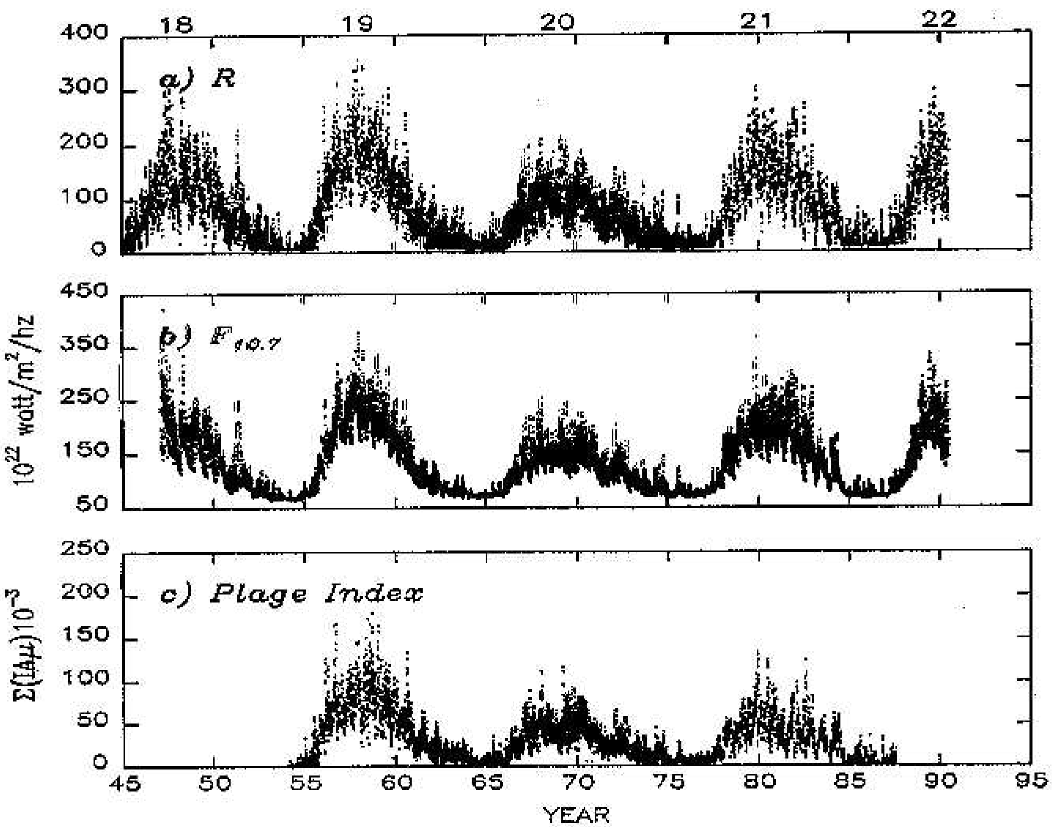
18
19
20
21
22
a) R
b) $F_{10.7}$
10^{22} watt/m^2/hz
c) Plage Index
$\Sigma(IA\mu)10^{-3}$
YEAR

Figure 11

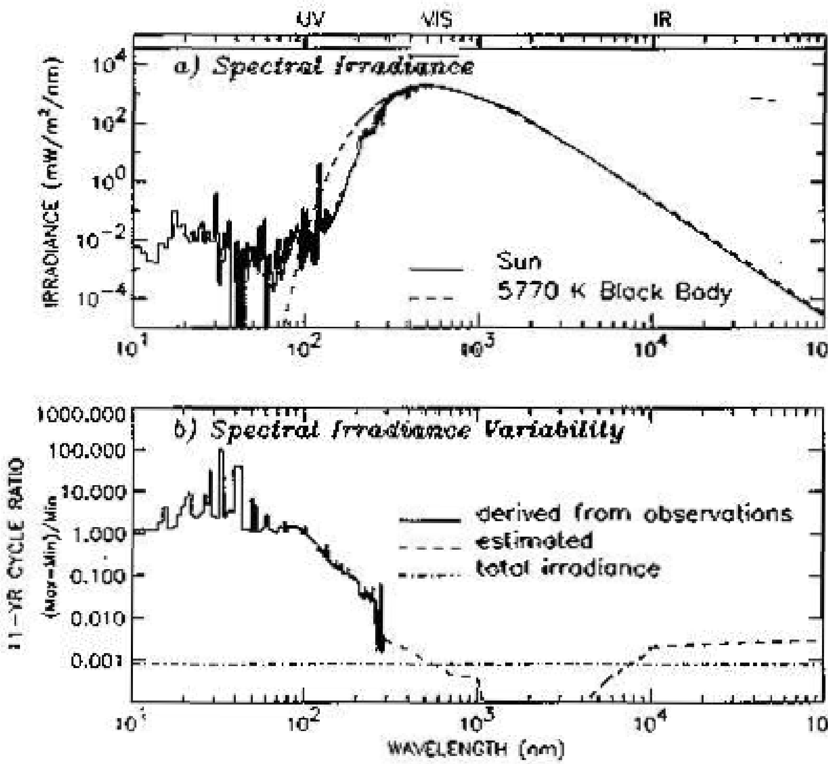

UV
VIS
IR
a) Spectral Irradiance
IRRADIANCE (mW/m²/nm)
Sun
5770 K Black Body
b) Spectral Irradiance Variability
11-YR CYCLE RATIO (Max-Min)/Min
derived from observations
estimated
total irradiance
WAVELENGTH (nm)

Figure 12

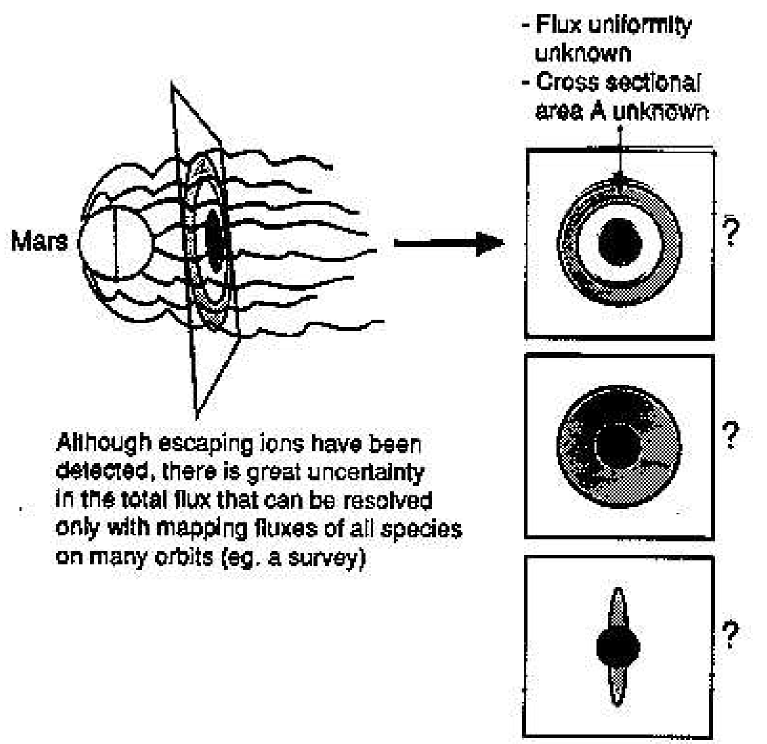
- Flux uniformity
unknown
- Cross sectional
area A unknown
Mars
?
?
?
Although escaping ions have been
detected, there is great uncertainty
in the total flux that can be resolved
only with mapping fluxes of all species
on many orbits (eg. a survey)

Figure 13

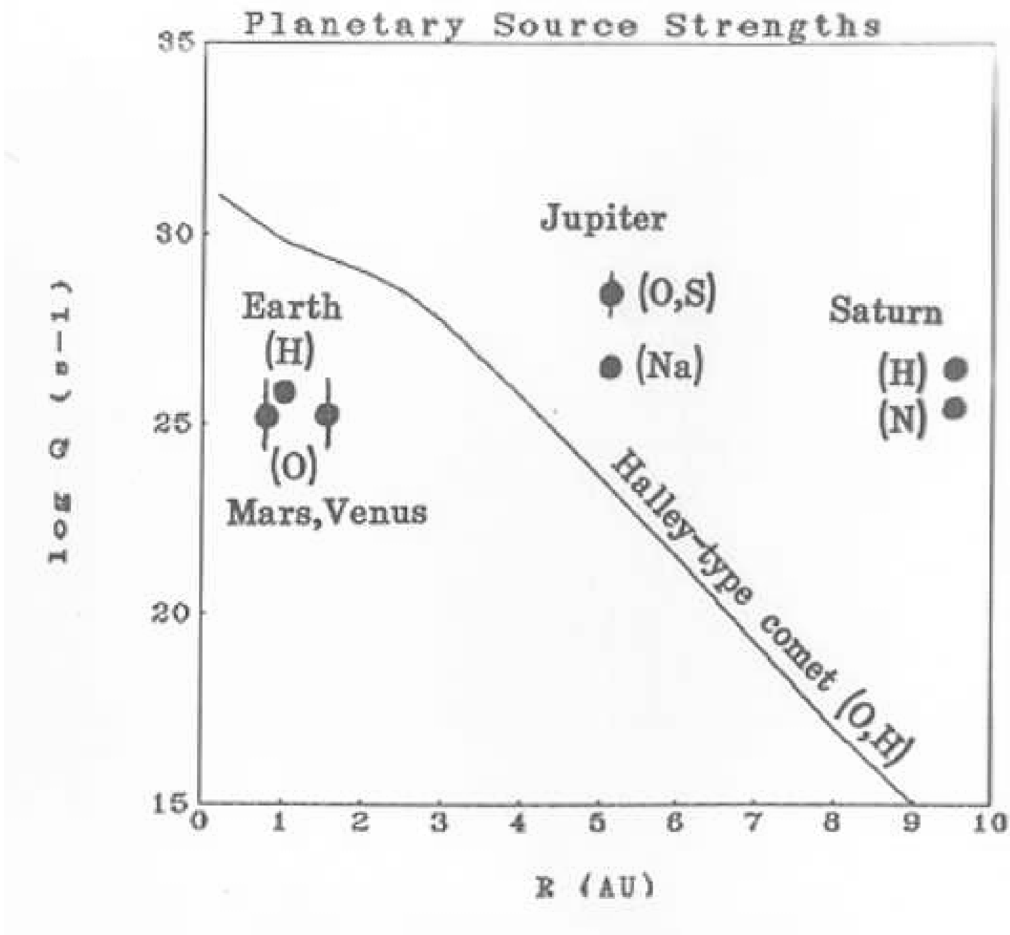

Planetary Source Strengths
35
30
25
20
15
0
1
2
3
4
5
6
7
8
9
10
log Q (s−1)
R (AU)
Earth
(H)
(O)
Mars,Venus
Jupiter
(O,S)
(Na)
Saturn
(H)
(N)
Halley-type comet (O,H)

Figure 14

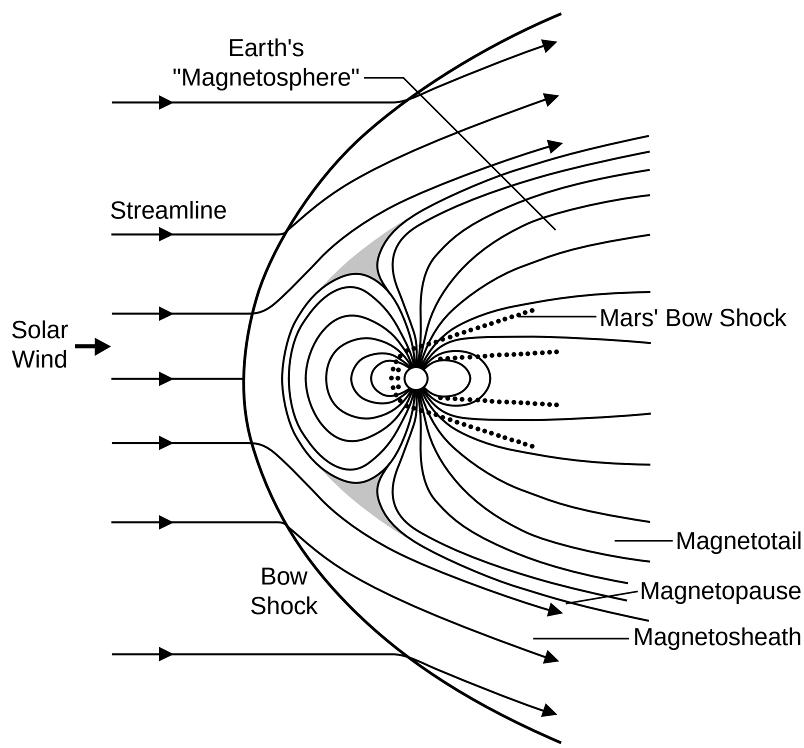
Earth's
"Magnetosphere"
Streamline
Solar
Wind
Mars' Bow Shock
Magnetotail
Bow
Shock
Magnetopause
Magnetosheath

Figure 15

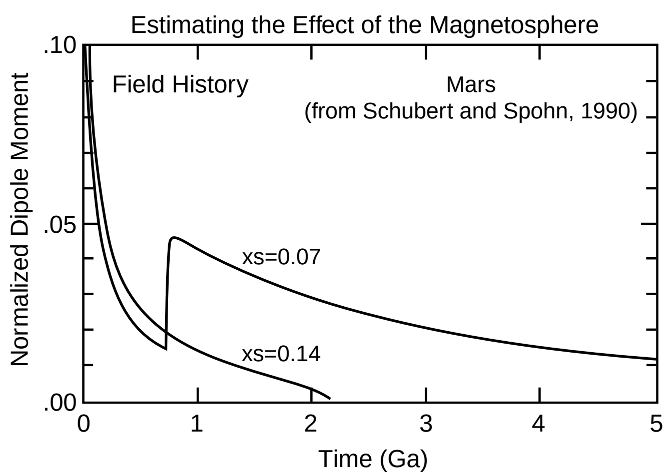
Estimating the Effect of the Magnetosphere
Field History
Mars
(from Schubert and Spohn, 1990)
xs=0.07
xs=0.14
Normalized Dipole Moment
.10
.05
.00
0
1
2
3
4
5
Time (Ga)

Figure 16

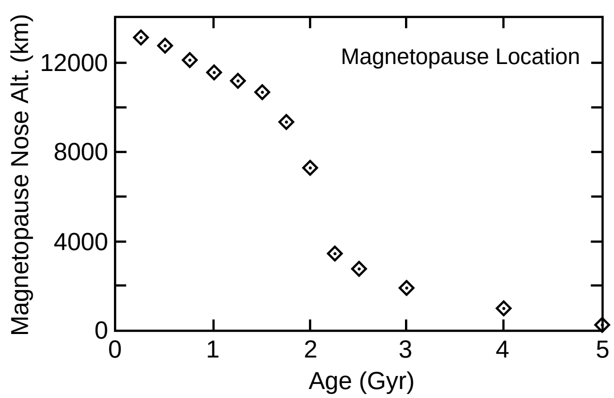
Magnetopause Location
Magnetopause Nose Alt. (km)
12000
8000
4000
0
0
1
2
3
4
5
Age (Gyr)

Figure 17

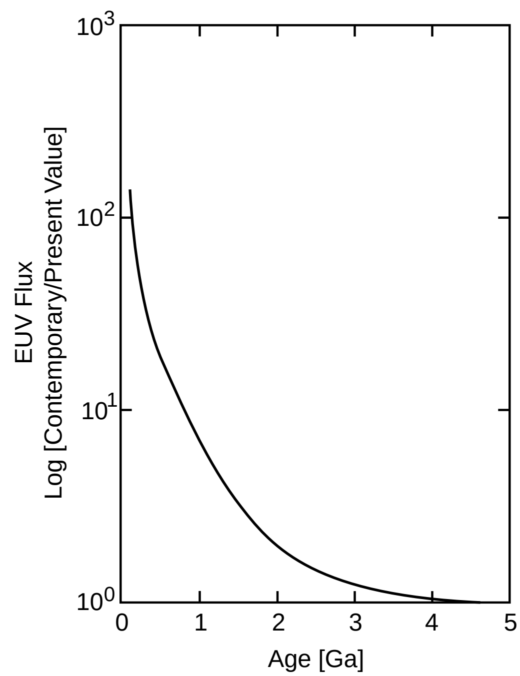

10^3
10^2
10^1
10^0
EUV Flux
Log [Contemporary/Present Value]
0
1
2
3
4
5
Age [Ga]

Figure 18

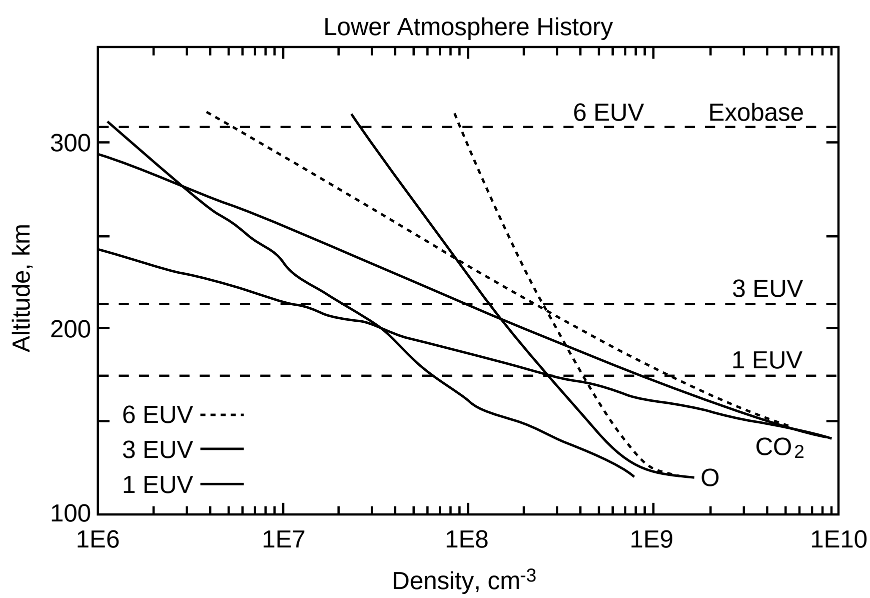
Lower Atmosphere History
6 EUV
Exobase
3 EUV
1 EUV
CO2
O
6 EUV
3 EUV
1 EUV
Altitude, km
300
200
100
1E6
1E7
1E8
1E9
1E10
Density, cm-3

Figure 19

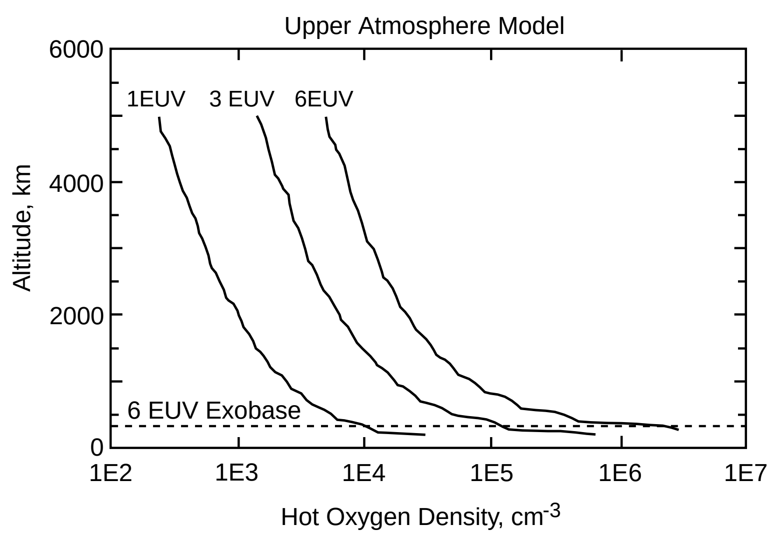

Upper Atmosphere Model
6000
4000
2000
0
Altitude, km
1EUV
3 EUV
6EUV
6 EUV Exobase
1E2
1E3
1E4
1E5
1E6
1E7
Hot Oxygen Density, cm-3

Figure 20

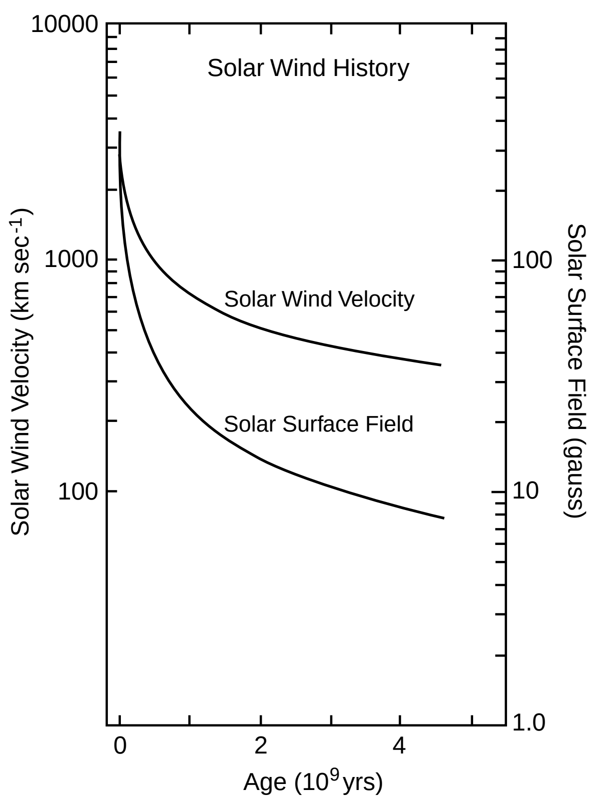
Solar Wind History
Solar Wind Velocity
Solar Surface Field
10000
1000
100
100
10
1.0
0
2
4
Age (10^9 yrs)
Solar Wind Velocity (km sec^-1)
Solar Surface Field (gauss)

Figure 21